Geoscience Frontiers xxx (2016) 1–21

HOSTED BY

ELSEVIER

Contents lists available at ScienceDirect

China University of Geosciences (Beijing)

Geoscience Frontiers

journal homepage: www.elsevier.com/locate/gsf

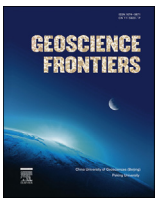

Research Paper

Monomineral universal clinopyroxene and garnet barometers for peridotitic, eclogitic and basaltic systems

I.V. Ashchepkov [a,*], T. Ntaflos [b], A.M. Logvinova [a], Z.V. Spetsius [c], H. Downes [d], N.V. Vladykin [e]

[a] V.S. Sobolev Institute of Geology and Mineralogy SB RAS, Novosibirsk, Russia
[b] Vienna University, A-1090 Vienna, Austria
[c] Alrosa Stock Company, Mirny, Russia
[d] Department of Earth and Planetary Sciences, Birkbeck University of London, London, UK
[e] Institute of Geochemistry SD RAS, Favorsky str. 1a, Irkutsk, 66403, Russia

ARTICLE INFO

Article history:
Received 13 October 2015
Received in revised form
2 June 2016
Accepted 13 June 2016
Available online xxx

Keywords:
Clinopyroxene
Barometer
Peridotite
Eclogite
Kimberlite
Garnet

ABSTRACT

New versions of the universal Jd-Di exchange clinopyroxene barometer for peridotites, pyroxenites and eclogites, and also garnet barometer for eclogites and peridotites were developed. They were checked using large experimental data sets for eclogitic (~530) and peridotitic systems (>650). The precision of the universal Cpx barometer for peridotites based on Jd-Di exchange is close to Cr-Tschermakite method produced by Nimis and Taylor (2000). Cpx barometer was transformed by the substitution of major multiplier for K_D by the equations dependent from Al-Na-Fe. Obtained equation in combination with the thermometer of Nimis and Taylor (2000) allow to reconstruct position of the magma feeder systems of the alkali basaltic magma within the mantle diapirs in modern platforms like in Vitim plateau and other Southern Siberia localities and several localities worldwide showing good agreement of pressure ranges for black and green suites. These equations allow construct PTX diagrams for the kimberlite localities in Siberia and worldwide calculating simultaneously the PT parameters for different groups of mantle rocks. They give very good results for the concentrates from kimberlite lamproites and placers with mantle minerals. They are useful for PT estimates for diamond inclusions. The positions of eclogite groups in mantle sections are similar to those determined with new Gar–Cpx barometer produced by C. Beyer et al. (2015). The Fe rich eclogites commonly trace the boundary between the lower upper parts of subcontinental lithospheric mantle (SCLM) at 3–4 GPa marking pyroxenite eclogites layer. Ca-rich eclogites and especially grospydites in SCLM beneath Precambrian kimberlites occurs near pyroxenite layer but in younger mantle sections they became common in the lower parts. The diamondiferous Mg Cr-less group eclogites referring to the ancient island arc complexes are also common in the middle part of mantle sections and near 5–6 GPa. Commonly eclogites in lower apart of mantle sections are remelted and trace the high temperature convective branch. The Mg- and Fe-rich pyroxenites also show the extending in pressure trends which suggest the anatexic melting under the influence of volatiles or under the interaction with plums.

1. Introduction

Clinopyroxene is common in most mantle rock-types including peridotites, eclogites, Cr-diopside and augite-bearing pyroxenites as well as in most metasomatic associations formed by interactions with plume- or subduction-related melts. Not all mantle rocks have the correct mineralogy to work with garnet–orthopyroxene barometry (Nickel and Green, 1985; Brey and Kohler, 1990) or orthopyroxene barometry (McGregor, 1974) which is thought to be

* Corresponding author. Sobolev's Institute of Geology and Mineralogy SD RASc, Academician V.A. Koptyug Avenue 3, 63090 Novosibirsk, Russia. Fax: +7 950 5918327; +7 383 2332792 (institute).
E-mail addresses: Igor.Ashchepkov@igm.nsc.ru, garnet@igm.nsc.ru, igora57@mail.ru (I.V. Ashchepkov).
Peer-review under responsibility of China University of Geosciences (Beijing).

http://dx.doi.org/10.1016/j.gsf.2016.06.012

the most reliable methods (Taylor, 1998; Wu and Zhao, 2011). However, monomineral single-grain clinopyroxene thermobarometry of Cr-bearing associations (Nimis and Taylor, 2000), based on the Cr-tschermakite has a broad range of applications in mantle petrology. Examples include studies of mantle metasomatism in orthopyroxene- and garnet-free associations (Nimis et al., 2009; Ziberna et al., 2013) in cratonic lithosphere and processes of refertillization in oceanic mantle. But this thermobarometer has some restrictions because it works only in Cr-rich rocks and is worse when applied to Fe-enriched and Al-Na-rich rock-types and is sensitive to Fe^{3+}.

The single pyroxene barometer (Ashchepkov, 2002; Ashchepkov et al., 2010, 2011) was developed to be more universally applicable and to investigate cumulates from basaltic and other Cr-poor magmas as well as eclogites and some Cr-poor but Na–Al-bearing pyroxenites. In the previous versions, three separate equations were applied to: (1) peridotites from alkali basalts representing relatively undepleted or close to primitive mantle compositions and basaltic cumulates; (2) more Al-depleted peridotites such as xenoliths in kimberlites; (3) mantle eclogites and pyroxenites.

In this paper we represent the universal version of the Jd-Di barometer which works simultaneously in most mantle systems. The method, together with the other most powerful and broadly used thermobarometric methods, has been combined in a PT program (Ashchepkov et al., 2011, 2013a). This program works using an iteration scheme calculating pressure and temperatures together. Since thermometers and barometers have mutual corrections, progressive iterations can produce quite different PT estimates compared to methods that calculate values in one step. For example the orthopyroxene barometer (McGregor, 1974) in combination with the Opx thermometer of Brey and Kohler (1990) gave much higher pressures for peridotites from Udachnaya and other kimberlite pipes.

The garnet monomineral barometer for peridotites (Ashchepkov, 2006; Ashchepkov et al., 2010, 2014) in its latest version shows very good agreement with the Opx-based estimates and has been transformed to be applicable also to eclogites. Compared with the original version (Ashchepkov, 2006), we made major modifications but this version is still preliminary because although it produces values similar to those produced by the Cpx barometer, it reproduces the experimental pressures rather poorly (55%). However it works for discrimination of diamond inclusions (Tsai et al., 1979; Logvinova et al., 2005). This is useful from the perspective of prospecting geologists because orange garnets may be used for both pressure estimates and estimation of the diamond grade.

The advantage of the universal clinopyroxene method is in good agreement with the experimental conditions for a large number of runs. For example many methods for eclogite and peridotite barometry are based on >30–50 experimental runs, whereas the universal clinopyroxene method is calibrated on >400 runs in peridotitic and >310 in eclogitic system. The correlations with the common barometers based on Opx (McGregor, 1974; Perkins and Newton, 1980) and Gar–Opx methods (Nickel and Green, 1985; Brey and Kohler, 1990) as well as with the Cpx method (Nimis and Taylor, 2000) are also good.

2. Data sets

For calibration, the natural compositions of xenoliths from alkali basalts in Vitim (~1600) and other localities from TransBaikal (Ashchepkov et al., 1989, 1991, 1996, 2003, 2002, 2011; Ashchepkov and Ionov, 1999) (~2200 all together) were used. From the literature we collected the microprobe analyses of minerals from garnet-bearing and other xenoliths from alkali basalts (Nixon and Boyd, 1979; Sen, 1988; Kopylova et al., 1995; Stern et al., 1999; Keshav et al., 2007; Ntaflos et al., 2007; Chen et al., 2001; Zheng et al., 2010).

The huge data base of microprobe analyses of minerals of xenoliths from Yakutian kimberlites (~37,000 association) analyzed by author (Ashchepkov et al., 2010, 2013a, 2014, 2016) was completed by data from dissertations (Ovchinnikov, 1990; Kuligin, 1997; Reimers, 1994; Malygina, 2000; Pokhilenko, 2006). All these analyses were made in IGM SD RAS using CambaxMicro and JeolSuperprobe microprobes and standard methods (Lavrent'ev et al., 1987) in the Analytic Centre of IGM SB RAS. In addition precise data were obtained using Cameca SX100 in the University of Vienna using parameters described previously (Ashchepkov et al., 2013b).

Xenolith data was obtained from the literature (Ionov et al., 2010; Goncharov et al., 2012; Yaxley et al., 2012). Literature data for peridotite and eclogite mantle xenoliths from many kimberlite localities worldwide were used also (see Ashchepkov et al., 2010, 2013a, 2014, 2016 and references therein).

For the more precise calibration of the clinopyroxene barometer, a number of experimental runs from 33 published papers devoted to eclogites and 27 to peridotites were used (see list in the Supplementary file 1).

3. Methods of calibration

The calibrations of both garnet and clinopyroxene barometers were firstly obtained from cross-correlations with the Opx-based (McGregor, 1974) pressure estimates (Ashchepkov, 2002, 2006). Natural compositions of clinopyroxene from xenoliths in kimberlites and alkali basalts including Cr-diopsides, omphacites and augites were used for the semi-empirical calibration of the Jadeite–Diopside internal clinopyroxene exchange: $CaMgSi_2O_6 = NaAlSi_2O_6$ with corrections for Fe (Ashchepkov, 2002, 2003). Then it was calibrated against the wider database in peridotitic (Ashchepkov et al., 2011) and eclogitic systems (Ashchepkov et al., 2014) with corrections for the all major components. Thermobarometers were recalibrated using the large databases for the peridotitic and eclogitic systems. The method of calibration differs from the common thermodynamic approach. The common thermodynamic equation ($P = a \times T°K \times \ln(K_D) + b \times \ln(T°K)/(c \times \Delta V) + d$) was transformed using empirical coefficients.

The thermodynamic parameters and activities were substituted by semi-empirical complex temperature dependent coefficients and equations working in a similar manner. For the garnet barometer, the number of transformations of the primary formulas by the introduction of these members increased the precision (Ashchepkov et al., 2010, 2015).

3.1. Universal clinopyroxene barometer

For clinopyroxene the simple $K_D = Na/Ca \times Mg/Al + Cr$ (Ashchepkov, 2002) was transformed to $K_D = Na/Ca \times Mg/(Al^{IV} + Cr - 2 \times Ti + Fe^{3+})$ (Ashchepkov, 2003). Further transformations with the introduction of temperature dependent components instead activities in K_D and complex free members instead of Margules parameters produced three separate pressure equations for the eclogitic and basaltic systems (Ashchepkov et al., 2010, 2011). The obtained $\Delta P = P_{calc} - P_{exp}$ values were studied for dependence on each component and their simple combinations. These corrections sometimes were dependent on temperature.

For the universal equation a new amendment was made with the major numeric multipliers behind K_D being replaced by a function dependent on Al, Na and FeO and $Fe^{\#}$. The simple temperature dependent multipliers were also introduced for Fe. Instead of three separate equations for the common peridotites,

Please cite this article in press as: Ashchepkov, I.V., et al., Monomineral universal clinopyroxene and garnet barometers for peridotitic, eclogitic and basaltic systems, Geoscience Frontiers (2016), http://dx.doi.org/10.1016/j.gsf.2016.06.012

pyroxenites and eclogites, the universal equation was produced. It operates slightly less precisely for shallow pressure peridotites but even better for eclogites and pyroxenites.

Final pressure equations for the eclogites, peridotites and pyroxenites are as follows:

$$P1 = MgO \times Cr_2O_3 \times (T°K - 1050) \times FeO/CaO \times TiO_2/7000$$

$$P2 = MgO \times Cr_2O_3 \times (T°K - 1200)/120000$$

$$Fe51 = Fe/[(Fe + Mg)/2] + 0.000045 \times (T°K - 790) - 0.022$$

$$AlCr = (Al - 0.01) \times ((T°K - 600)/700)^{0.75} + Cr \times (T°K - 100)/1000 + (4 \times Ti - 0.0125)/(T°K - 801) \times 650 + 0.55 \times (Fe - 0.23) \times (T°K - 900)/10000 - K;$$

$$P(kbar) = 0.275 \times (4 + (8.75 \times Al + 1.25 \times Na + Na - 0.035 \times Cr/Al \times Ti) \times 5.75 - 1.75 \times Fe/(Fe + Mg) + 0.125) \times KD \times T°K^{0.75}/(1 + Fe + Fe \times (T°K - 600)/1250) - \ln(1273/T°K) \times 40 \times (7 \times Na - Al - 15 \times Ti + 10 \times Cr + Mg/4) + 7.5 \times Si - 20 \times Al \times Na \times Mg/Ca/(Al - 2 \times Ti + 2 \times Na - 2.5 \times Fe^{3+}) + 50 \times Na + 0.2 \times Al - 2 \times Ti + 0.075 \times Mg - 0.22 \times Ca - 0.75 \times Na)/Ca)$$ (for eclogites)

$$P(kbar) = 0.275 \times (4 + (8.04 - Na \times (Al + (Na - 0.035) \times Cr/Al \times Ti \times 5.75 + 1.25Na - 2 \times Fe/(Fe + Mg) + 0.125) \times K_D \times T°K^{0.75}/(1 + Fe + Fe \times (T°K - 550)/1300) - \ln(1273/T°K) \times 40 \times (7 \times Na - Al - 15 \times Ti + 10 \times Cr + Mg/3) + 7.5 \times Si - 20 \times Al \times Na \times Mg/Ca/(Al - 2 \times Ti + 2 \times Na - 2.5 \times Fe^{3+}) + 50 \times (Na + 0.2 \times Al - 2 \times Ti + 0.075 \times Mg - 0.22 \times Ca - 0.75 \times Na)/Ca)$$ (for pyroxenites)

where Si, Ti, Al, Cr, Fe, Mn, Mg, Na and K are elements in formular units; AlCr is approximation of Al, Cr and Ti activity together in M2 position in clinopyroxene structure; P(kbar) −pressure in kbars; T°K −temperature in Kelvin's.

3.2. Universal garnet barometer

In the first version, the common dependence of the knorringite and uvarovite components in the Fe-free system (Sobolev et al., 1973; Doroshev et al., 1997; Grütter et al., 2006; Turkin and Sobolev, 2009) with corrections for all other components and separate corrections for FeO and other components were used (Ashchepkov, 2006). New introductions were made for Fe-rich rock-types. The barometer consists of several equations and iterations taken from computer program (see description in Appendix) which were introduced after comparison with the experimental PT values. Pressure is in kbars and oxide components in wt.%.

$$xd = (CaO + MnO + 2 \times FeO)^{0.4}$$

$$P = 5.25 \times Cr_2O_3/xd + 0.02 \times (T°K - 273) + 22.5 \times Na_2O + MgO/20 + 0.5 \times CaO - TiO_2 - 12 + FeO/7$$

$$P = P \times 2.05 + 0.0045 \times P$$

$$P = -0.00007 \times P^3 + 0.0057 \times P^2 + 0.87 \times P$$

$$P = P + 5.5 \times Na_2O + MgO/FeO$$

$$P = P - (4 - Cr_2O_3) \times 0.9 - (TiO_2 - 0.1) \times (10 - FeO - 7) \times 2$$

The improvements comparing to the previous version (Ashchepkov, 2006) are as follows:

For peridotites:

$$P = 0.855 \times P + 0.485/CaO \times T°K/1050 + TiO_2 \times 200$$

$$P = (P - 40)/(T°K - 1000)/FeO \times 10 + P$$

$$P = P + P1 \times Fe51 \times 5 + P2 \times (1 - Fe51)$$

$$P = P - 6 \times Cr/Ca \times 2 - 12.6 \times CrCa + 25 - 5 \times TiO_2$$

For eclogites the Na- admixture after Sobolev and Lavrent'ev (1971) and Ca/(Ca + Mg) after Bobrov et al. (2009) are used:

$$P = 0.815 \times P + 0.45 \times CaO \times T°K/1150 + TiO_2 \times 200$$

$$P = (P\text{-}15 + Na_2O/TiO_2 \times 1.75 + CaO/MgO \times 13.5 + CaO/FeO \times 3.25) \times 1.51 + 8.15 \times Na_2O/CaO + 7.25 \times Na_2O/FeO + 8.15 \times TiO_2/Na_2O - 120 \times MnO \times Na_2O - 50 \times Fe/(Fe + Mg)$$

$$P = P + (xv(5,7) - 11) \times 1.25 - (xv(5,8) - 8.75) \times 2.8$$

$$P = (P - 55) \times 0.87 + 57$$

$$P = P \times 0.9$$

4. Precision of the barometric methods

4.1. Comparison with experimental data in peridotite system

The correlations of the pressure estimates using experimental data sets for peridotitic systems were obtained using ~600 experimental runs in which only ~350 contain garnet, orthopyroxene and clinopyroxene which can produce the correct Gar−Opx barometric and Cpx−Opx thermometric calculations. Our experimental database contains many recent studies (Wang et al., 2010; Kiseeva et al., 2012; Bulatov et al., 2014; Girnis et al., 2013; Sharygin et al., 2015; Sokol et al., 2016) for high pressures and complex systems (see list in Supplementary file 1) compared with those used in previous works (Taylor, 1998; Wu and Zhao, 2011). Those runs which produced results far from the pressure ranges in all thermobarometers were removed from the database. The comparisons of our three peridotite barometers, i.e. the universal Cpx barometer, Cpx barometer for peridotites, Gar barometer for peridotites, are shown on the Fig. 1A, B, and I. The universal Cpx

Please cite this article in press as: Ashchepkov, I.V., et al., Monomineral universal clinopyroxene and garnet barometers for peridotitic, eclogitic and basaltic systems, Geoscience Frontiers (2016), http://dx.doi.org/10.1016/j.gsf.2016.06.012

barometer (Ashchepkov et al., 2015) showed a better correlation with the experimental values giving good estimates for 439 runs and the peridotite barometer (Ashchepkov et al., 2011, corrected) (see equation in Appendix) for 419 runs.

The Gar–Opx barometers (Harley, 1984; Nickel and Green, 1985; Nickel, 1989; Brey and Kohler, 1990; Fig. 1E, F, G, and H) reveal slightly less good agreement with the experimental values. The results of Brey and Kohler (1990) and Nickel and Green (1985) are better than the others. The Opx barometer (Fig. 1D; McGregor, 1974) also gives better results than that of Nimis and Taylor (2000) (Fig. 1G).

4.2. Comparison with experimental data in eclogite system

Published Gar–Cpx barometers for mantle eclogites (Brey et al., 1986; Mukhopadyay, 1991; Simakov, 2008; Beyer et al., 2015) mainly use the Ca-Tschermakite component, calibrated sometimes on rather restricted data sets not > 60 experimental runs (Simakov, 2008), while the database used in this paper uses >600 runs. Not all of them include both garnets and clinopyroxenes. The best of them (Beyer et al., 2015) give rather good correlation for 190 experimental runs to 70 kbars. But its application to natural rock-types is

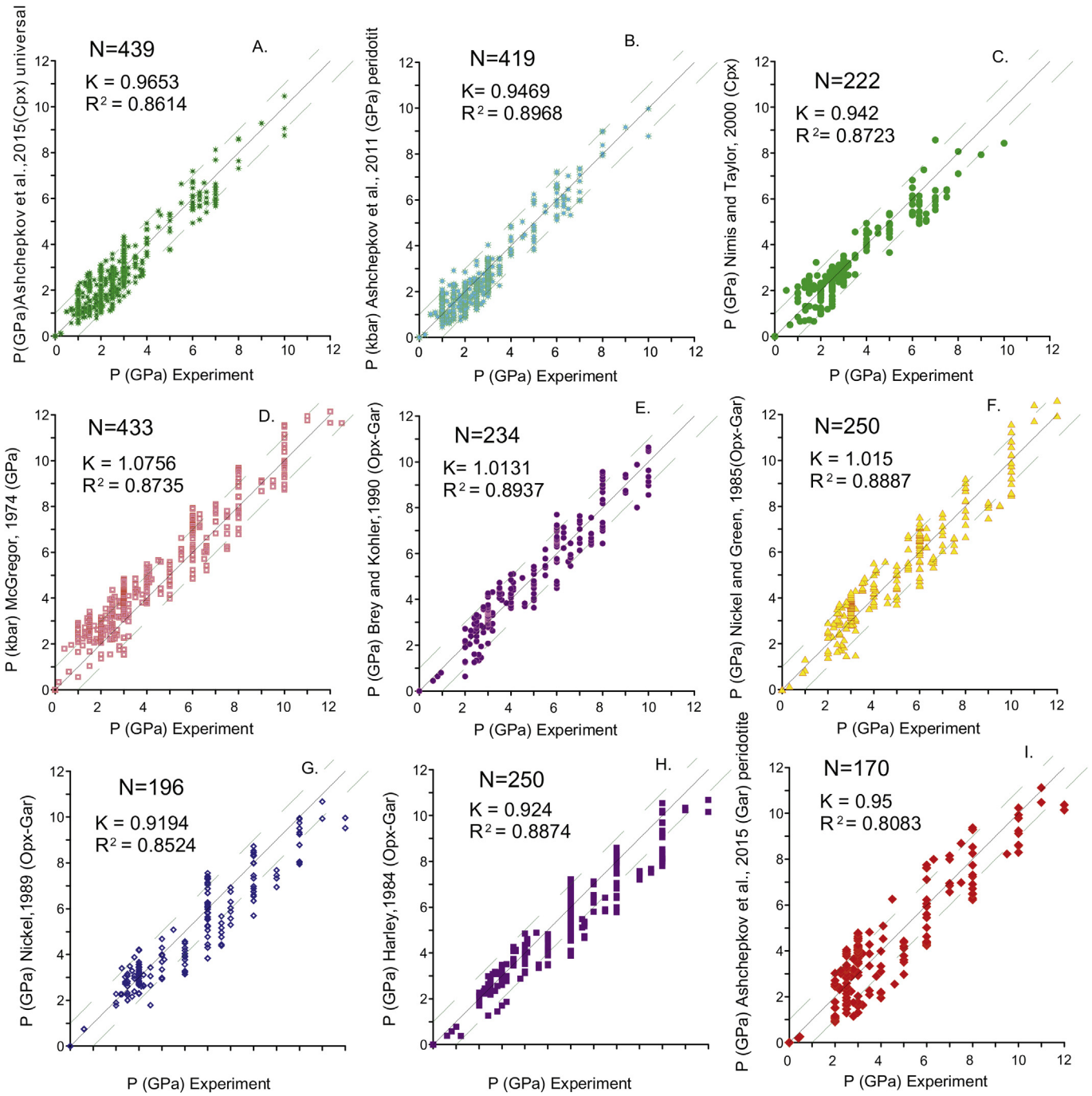

Figure 1. Correlation diagrams for pressure estimates obtained by mineral barometric methods and values of pressures in experiments (in GPa). Cpx methods: (A) P_{Exp}– P (Ashchepkov et al., 2015; UnCpx); (B) P_{Exp}– P (Ashchepkov et al., 2011; for peridotites); (C) P_{Exp}– P (Nimis and Taylor, 2000; Ashchepkov et al., 2015; Gar). For orthopyroxene: (D) P_{Exp}– P (McGregor, 1974). For Opx-Gar: (E) P_{Exp}– P (Brey and Kohler, 1990); (F) P_{Exp}– P (Nickel and Green, 1985); (G) P_{Exp}– P (Nickel, 1989); (H) P_{Exp}– P (Harley, 1984); (I) P_{Exp}– P (Ashchepkov et al., 2015; for peridotite Gar).

Please cite this article in press as: Ashchepkov, I.V., et al., Monomineral universal clinopyroxene and garnet barometers for peridotitic, eclogitic and basaltic systems, Geoscience Frontiers (2016), http://dx.doi.org/10.1016/j.gsf.2016.06.012

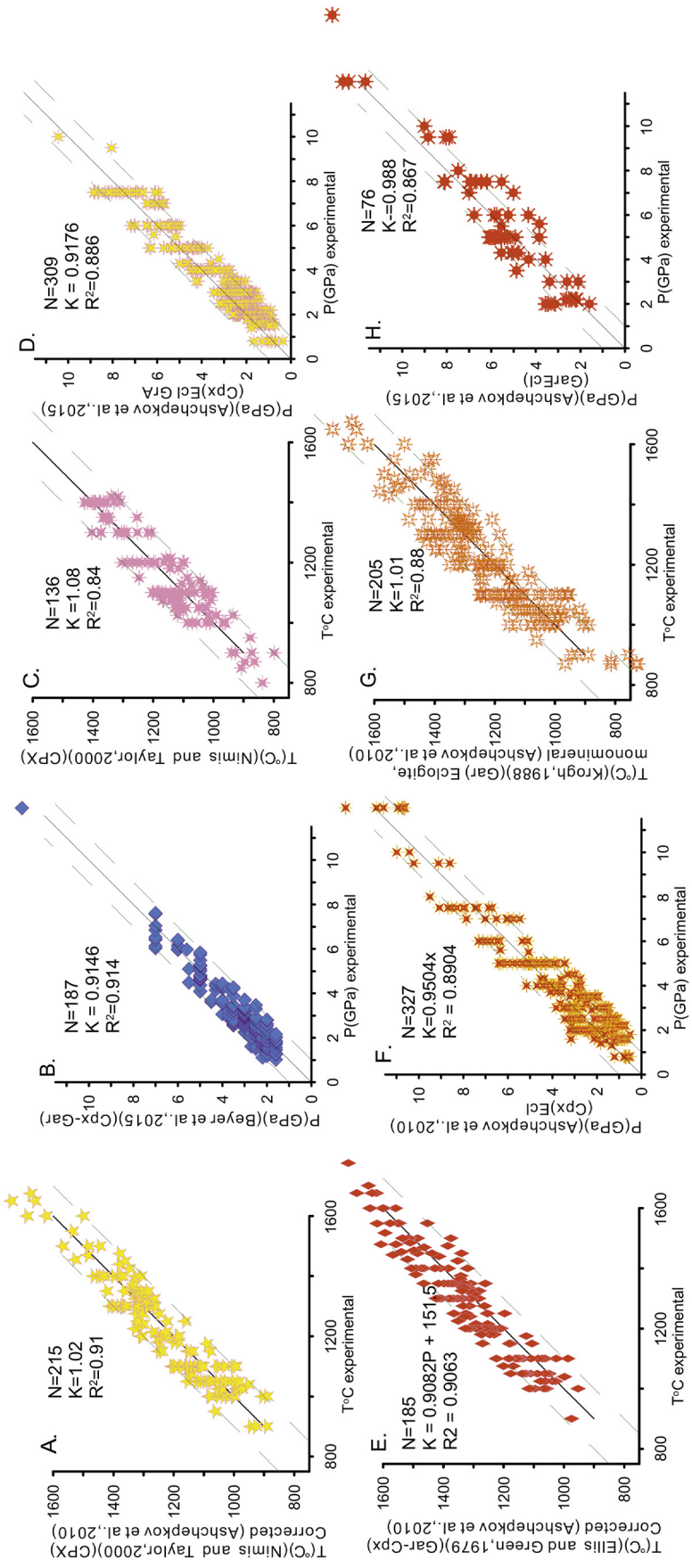

Figure 2. Correlations of the temperatures and pressures for eclogites using experimental runs. Temperatures determined with thermometers: (A) $T°C_{exp} - T°C$ (Nimis and Taylor, 2000) corrected; (C) $T°C_{exp} - T°C$ (Nimis and Taylor, 2000); (E) $T°C_{exp} - T°$ (Ellis and Green, 1979); (G) $T°C_{exp} - T°C$ (Krogh, 1988). Pressures (in GPa) determined with Cpx: (B) $P_{exp} - P$ (Beyer et al., 2015); (D) $P_{exp} - P$ (Ashchepkov et al., 2015; Univ); (F) $P_{exp} - P$ (Ashchepkov et al., 2010); (H) $P_{exp} - P$ (Ashchepkov et al., 2015; GarEcl).

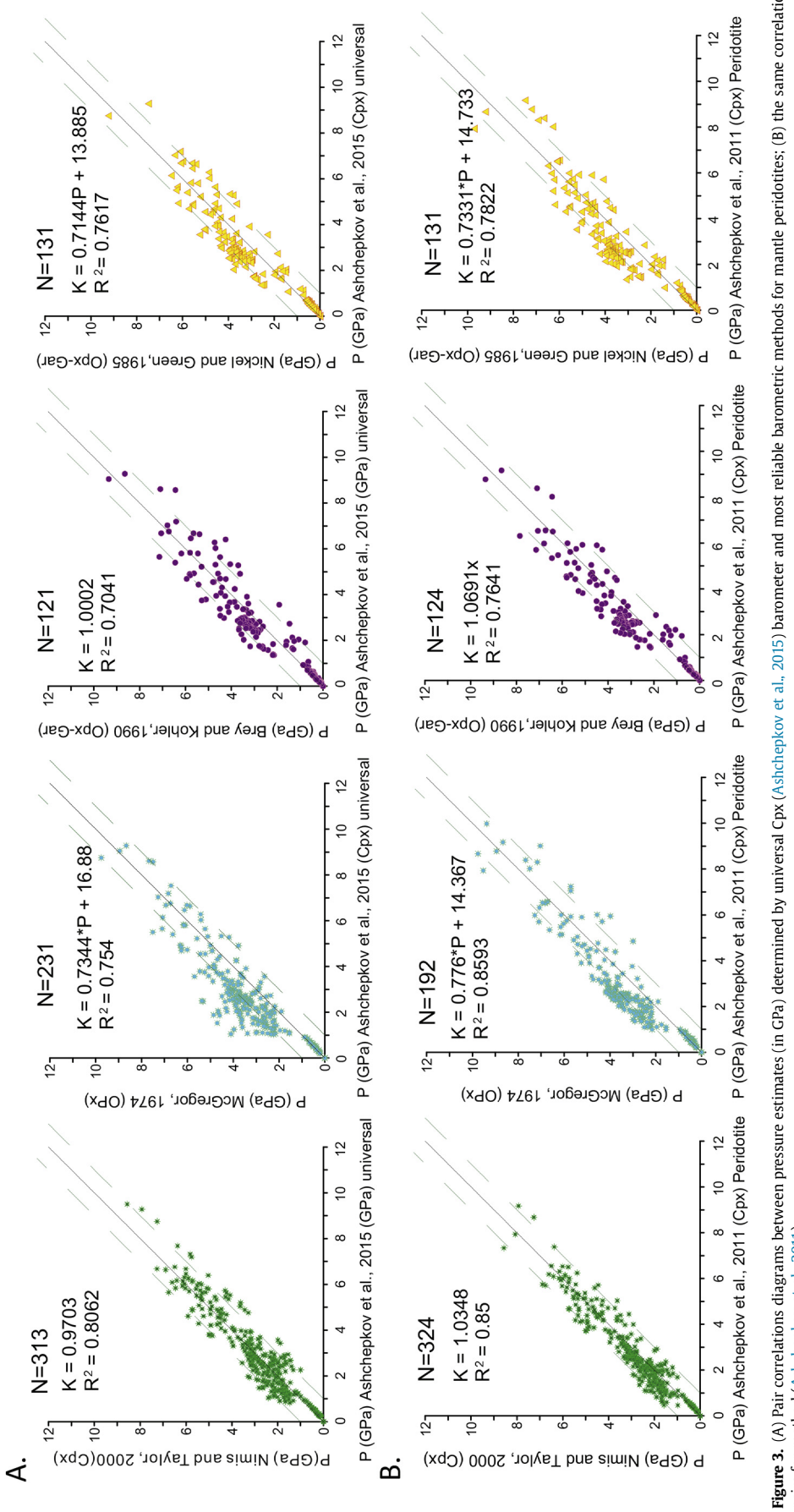

Figure 3. (A) Pair correlations diagrams between pressure estimates (in GPa) determined by universal Cpx (Ashchepkov et al., 2015) barometer and most reliable barometric methods for mantle peridotites; (B) the same correlation pairs for method (Ashchepkov et al., 2011).

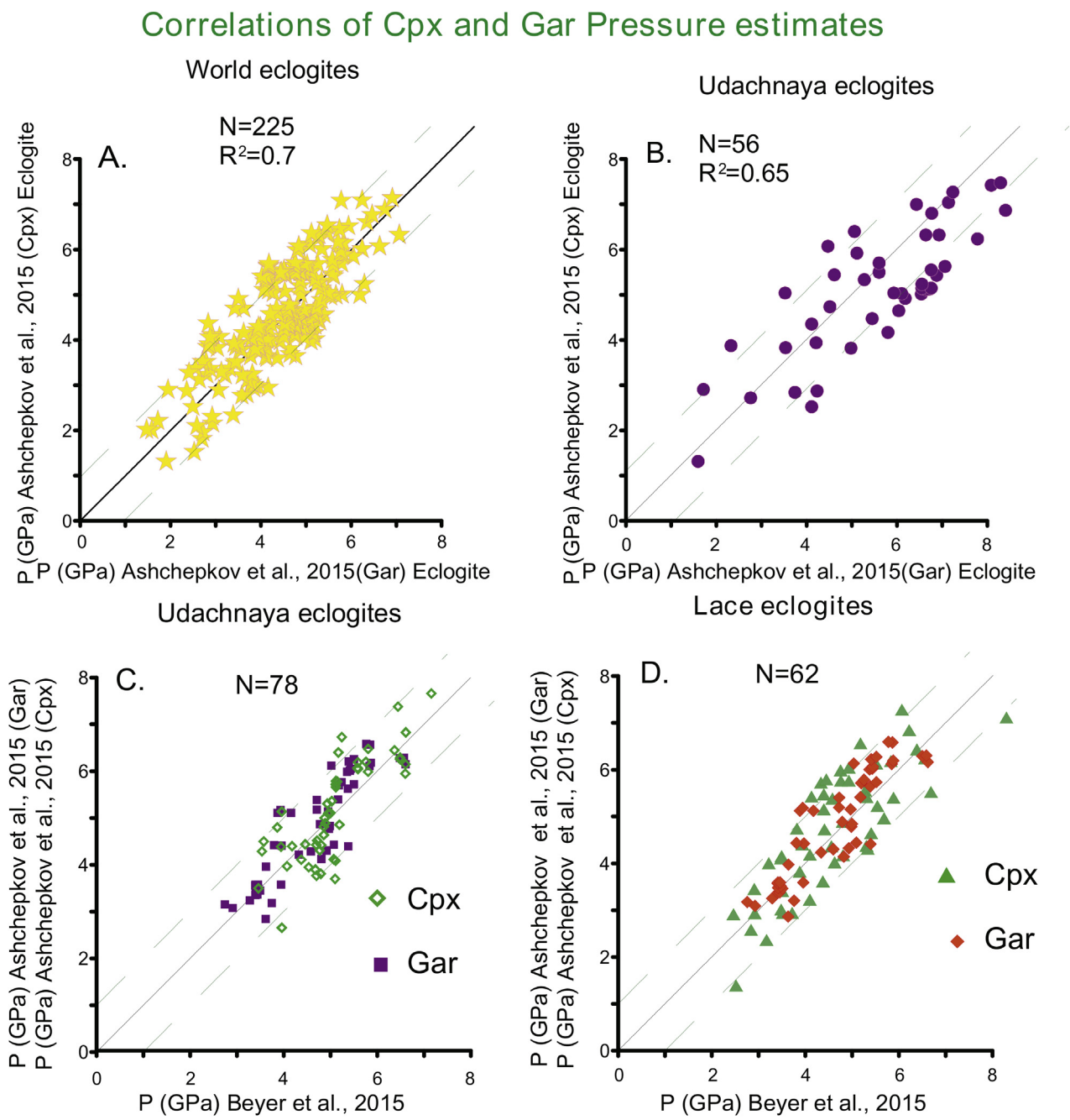

Figure 4. Comparison of the PT estimates for Udachnaya mantle section using the Opx-based methods (Brey and Kohler, 1990; Opx).

sometimes not easy because it is very sensitive to Si in the formula. Many microprobe analyses of eclogites show an excess of Si (>2) (Kopylova et al., 2016). This method is also sensitive to the temperature estimates much more than the method of Ashchepkov et al. (2015).

In the eclogite system, the pressures estimated with new Gar–Cpx barometer (Beyer et al., 2015) give rather good correlation (for 187 runs, $R^2 \sim 0.91$) with the pressure values in experiments to 7 GPa (Fig. 2B). Method need good analyses for Si in Cpx. The universal Cpx barometer of Ashchepkov et al. (2015) give a linear correlation for 310 runs (>80% of all calculated values) with rather low dispersion ($R^2 \sim 0.9$) using both the methods of Ashchepkov et al. (2015) and eclogitic version of the Cpx barometer of Ashchepkov et al. (2010) (Fig. 2D and F). The garnet eclogite barometer (Ashchepkov et al., 2015) is very preliminary and shows poorer correlations with the experimental values (Fig. 2H). But it shows a correlation with the PT estimates produced by clinopyroxenes for Udachnaya (Sobolev et al., 1994; Kuligin et al., 1997; Shatsky et al., 2008) and Lace eclogites (Aulbach and Viljoen, 2016; Aulbach et al., 2016) and worldwide eclogite xenoliths from kimberlites (Fig. 4A and B). It also gives a moderately good correlation with the pressure estimates obtained with the Gar–Cpx barometer (Beyer et al., 2015; Fig. 4C and D).

4.3. Comparison with the most reliable barometers

The correlation diagrams of the obtained pressures with the experimental conditions for >600 associations (Fig. 1) are in

general similar to those previous publications (Wu and Zhao, 2011). The new correlation diagrams give more details in the high pressure field as shown by the correlation coefficients and numbers of the estimates within the confidence interval (1 GPa). The method of Ashchepkov et al. (2015) (Fig. 2A) shows a better correlation then previous version (Ashchepkov et al., 2011) (Fig. 2B) mainly because it works for a wider compositional range compared with the method of Nimis and Taylor (2000). The correlation with the values determined with the Opx barometer of McGregor (1974) shows an inclined trend line which overestimates the low pressure part. Nearly the same is observed in the correlations of Ashchepkov et al. (2015) with the methods of Brey and Kohler (1990) and Nickel and Green (1985), but the latter shows less dispersion. Nevertheless, the agreement of the Cpx Jd–Di methods with the reliable mantle barometers is good enough to obtain realistic PTX diagrams for mantle column in wide pressure ranges and compositions.

In the peridotite system, the correlations of pressure estimates of universal Cpx barometer of Ashchepkov et al. (2015) with the other methods (Fig. 3) also show a better correlation with the method of Nimis and Taylor (2000). The previous peridotite–pyroxenite barometer of Ashchepkov et al. (2011) works better for the peridotites especially in low pressure field and is better for xenoliths from alkali basalts. The data of the calculations are given in Supplementary files 2–4.

Garnet and clinopyroxene estimates using the universal Cpx and Gar barometers for eclogites commonly show good mutual agreements for the same rock-type, although many eclogites from worldwide kimberlites (Fig. 4A) and Udachnaya pipe (Fig. 4B) are not equilibrated (Shatsky et al., 2008). The Gar–Cpx barometer

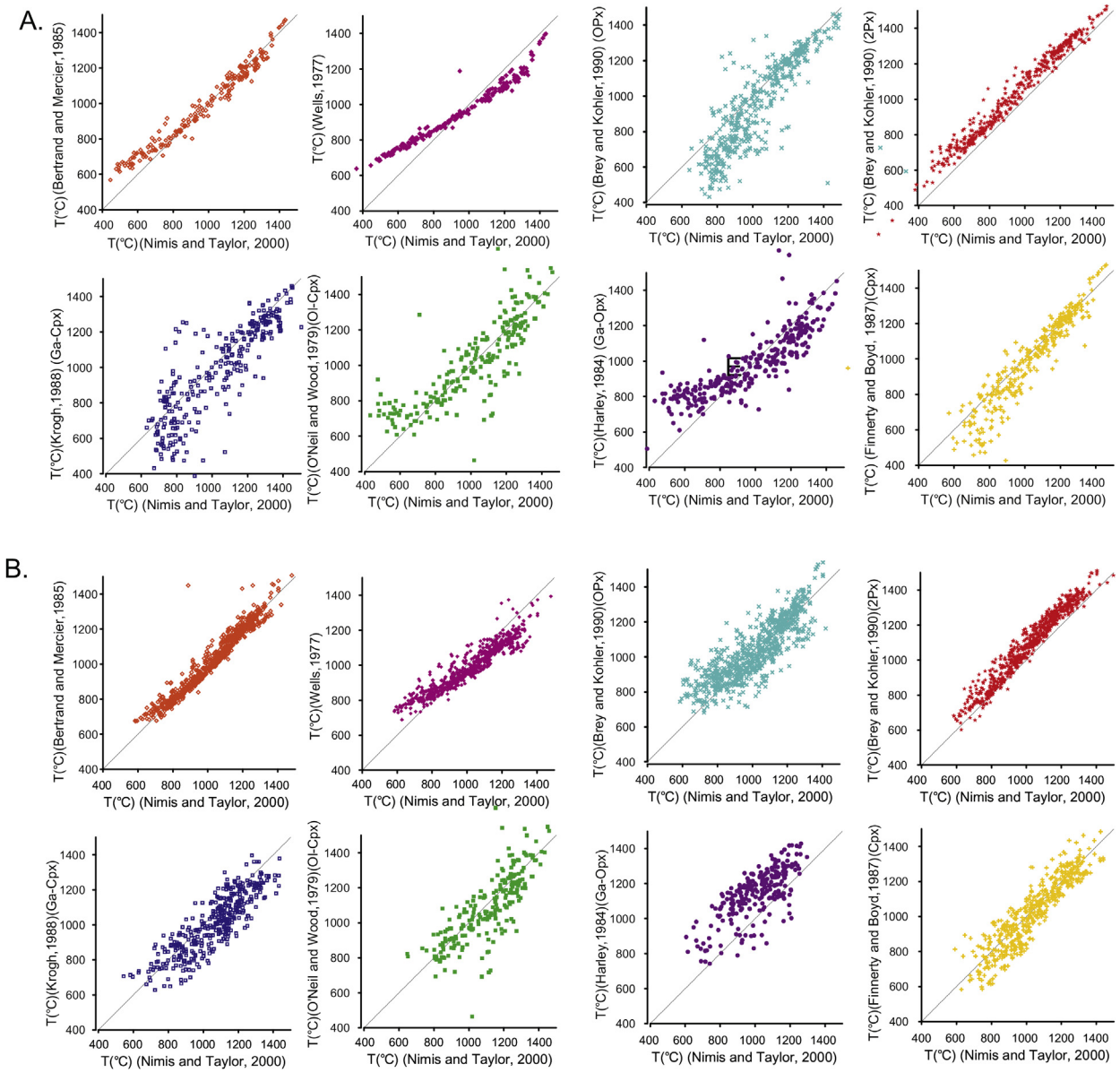

Figure 5. Pair correlations diagrams between (A) Cpx (Nimis and Taylor, 2000) thermometer and most reliable thermometric methods for mantle peridotites (Wells, 1977; O'Neill and Wood, 1979; Harley, 1984; Bertrand and Mercier, 1985; Finnerty and Boyd, 1987; Krogh, 1988; Brey and Kohler, 1990; Opx, 2Px); (B) the same for the corrected version which enhanced the agreement.

Please cite this article in press as: Ashchepkov, I.V., et al., Monomineral universal clinopyroxene and garnet barometers for peridotitic, eclogitic and basaltic systems, Geoscience Frontiers (2016), http://dx.doi.org/10.1016/j.gsf.2016.06.012

(Beyer et al., 2015) shows a moderately good correlation with the experimental pressures (Fig. 2E).

4.4. Comparison with the most reliable thermometers

The influence of the temperature in the formula is also very important, because the joint solution of the temperature and pressure equation using iteration procedure can yield a major difference in the final result compared with the first iteration values. In this case, the method of Brey and Kohler (1990) is better, while the method of Nimis and Taylor (2000) is more appropriate. The methods of McGregor (1974) and universal Cpx of Ashchepkov et al. (2015) show much more dependence on temperature. Choice of the wrong method for the temperature estimates could cause major errors in the resulting pressures.

The temperatures in the monomineral clinopyroxene barometer are calculated using Cpx monomineral thermometer of Nimis and Taylor (2000) with corrections (Ashchepkov et al., 2010) which yield better agreement with the experimental values and the temperature estimates made by the best thermometers for the mantle peridotites. Nevertheless, in any case, it produces lower temperature values. In this version corrections are as follows:

$$T°K = -0.000001 \times T°K^2 + 0.95 \times T°K + 33.75 \times (Al_2O_3 + Cr_2O_3) - 55 - 17.9 \times (FeO - 2.5) - 10.9 \times Na_2O$$

and then for Cr low Cpx: $T°K = (T°K + 390) \times P/(P - 70) \times 0.95$.

This produces good agreement with the experimental temperatures for eclogites and peridotites. Looking at the correlation diagrams, the correlations of primary NT2000 methods is lower (Fig. 5A) than those obtained after the corrections (Fig. 5B) especially for the Brey, Kohler Opx and two-pyroxene and the methods from Bertrand and Mercier (1985).

5. Discussion

5.1. Mantle xenoliths from Vitim basalt plateau

The Cpx universal method demonstrates very good application for mantle xenoliths in alkali basalts, allowing us to see the joint development of the mantle column and feeder system for the basaltic magmas traced by the augite megacrysts.

The mantle lithosphere beneath the Vitim basaltic plateau formed in several stages from 20 to 0.6 Ma (Ashchepkov et al., 2002, 2003, 2011) as demonstrated by the PT diagrams for four of the stages. The PT estimates show that modifications of the mantle columns were associated with the evolution of large magmatic systems, which changed (Johnson et al., 2005) from picrobasalts in the initial middle Miocene stage (Fig. 6A) to basanite in the upper Miocene stage (Fig. 6B), Ne-hawaiite in the Pliocene stage (Fig. 6C) and mugearites in the Pleistocene stage when the Kandidushka volcano was formed (Fig. 6D) (Ashchepkov et al., 2003). The pyroxenites were formed during the development of systems of magmatic channels and chambers with black and green Cr-poor Gar pyroxenites in the lower levels and Pl-bearing assemblages in the upper levels. Associated veins in peridotites evolved in mantle columns from the black water-free pyroxenites to kaersutite–phlogopite-bearing Gar pyroxenites (Ashchepkov, 1991; Glaser et al., 1999). Comparison of the reconstructed mantle section in different stages of lithospheric evolution beneath the Vitim Plateau demonstrates that geotherms have an advective nature. High-T peridotites from the later stages give PT-trends which coincide with those of the megacrystalline pyroxenites from the earlier stages. The PT-paths from the three separate stages slightly vary in depth and only in the upper Miocene stage correspond to the upper part of spinel facies. The geotherms show relative decreases in temperature. The detailed investigations of mantle structure and layering vary from stage to stage showing the changes in the mineralogical features of the mantle column (Ashchepkov et al., 1989, 2002; Glaser et al., 1999), which suggest vast interaction of magmatic liquids with peridotites and melt percolation through the peridotite mantle (Ashchepkov et al., 2011), probably accompanied by mantle diapirism. In the period of the lava plateau formation, mantle xenoliths captured by the ascending magmas from the upper part of the mantle column show no sign of heating or strong interaction with basaltic melts. In the latest stages, the amount of garnet peridotites at the same depth decreased compared to the first stage. At the stages of valley basalts and cinder cones, the green pyroxenites with relics of garnets were transported to the spinel facies probably due to mantle diapirism. Black garnet-bearing megapyroxenites also became rare and often show signs of deformation. Megacrysts of Cpx and Gar have geochemical features similar to basalts. Most of them originated from more differentiated melts than basalts and show relatively high contamination by peridotite material which was much greater in the first stage and diminished at the last stage. The capturing intervals also varied with time, being deeper in the first stage. Nevertheless, signs of mantle upwelling are also pronounced. The prevailing garnet peridotites from the picrite basalt stage are from depleted mantle (Ionov et al., 2005) concentrated in the deeper part and thus should be uplifted as the mantle diapir developed in the Oligocene (or earlier as inferred from Sm–Nd data 45–25 Ma) (Ionov et al., 2005). Our $^{40}Ar-^{39}Ar$ ages for phlogopite are also close. Diapiric uprise was accompanied by partial melting and left a lot of garnet-bearing Cr-rich pyroxenites, though part of them may be also associated with the later interaction with hydrous picrite basalt melts (Glaser et al., 1999). In the stage of valley basalts, similar pyroxenites show signs of garnet decomposition, possibly due to mantle upwelling, whereas such rocks are practically absent among the xenoliths of the last stage.

5.2. Southern Siberia basalt localities

The *Burkal basalt locality* in the Khantay range (Ashchepkov et al., 1996) contains fertile garnet peridotite xenoliths which give a geotherm slightly above "oceanic" (90 mW/m^2) in the deep part of capture interval, while the upper part is composed of more depleted spinel peridotites (Fig. 7A). The megacrysts show three separate pressure intervals and evolution from the Cr-bearing Mg-rich suite to the Fe-rich and Cr-poor varieties with $Fe^{\#} = Fe/(Fe + Mg) = 0.15 - 0.33$.

In the *East Sayan mountain range* (Ivanov et al., 2008) mainly fertile peridotite xenoliths with relic garnet were studied. They have a lower heating degree and lie on a geotherm located slightly below 90 mW/m^2. Augite megacrysts also show evolution within the 1.7–1.0 GPa pressure interval (Fig. 7B).

Bartoy basalt volcano locality in the southern part of Khamar–Daban contains a huge range of variety of xenoliths (Ashchepkov and Ionov, 1999) starting from garnet–Cpx kaersutites with Phl to Cpx–Pl assemblages (Ashchepkov and Ionov, 1999) within 1.7–1.0 GPa interval (Fig. 7C). Surrounding peridotites were affected by metasomatism as shown by phlogopite and pargasite crystallization which was likely produced by evolving hydrous protobasaltic melts during formation of the melt feeder system.

Minusa alkali basalt pipes (Ashchepkov et al., 1995) of late Cretaceous age (74–82 Ma) (Metelkin et al., 2007) also contain garnet-bearing peridotites. They relate to a refertilization event and represent a rather shallow depth interval (1.5–1.8 GPa) and reflect

Please cite this article in press as: Ashchepkov, I.V., et al., Monomineral universal clinopyroxene and garnet barometers for peridotitic, eclogitic and basaltic systems, Geoscience Frontiers (2016), http://dx.doi.org/10.1016/j.gsf.2016.06.012

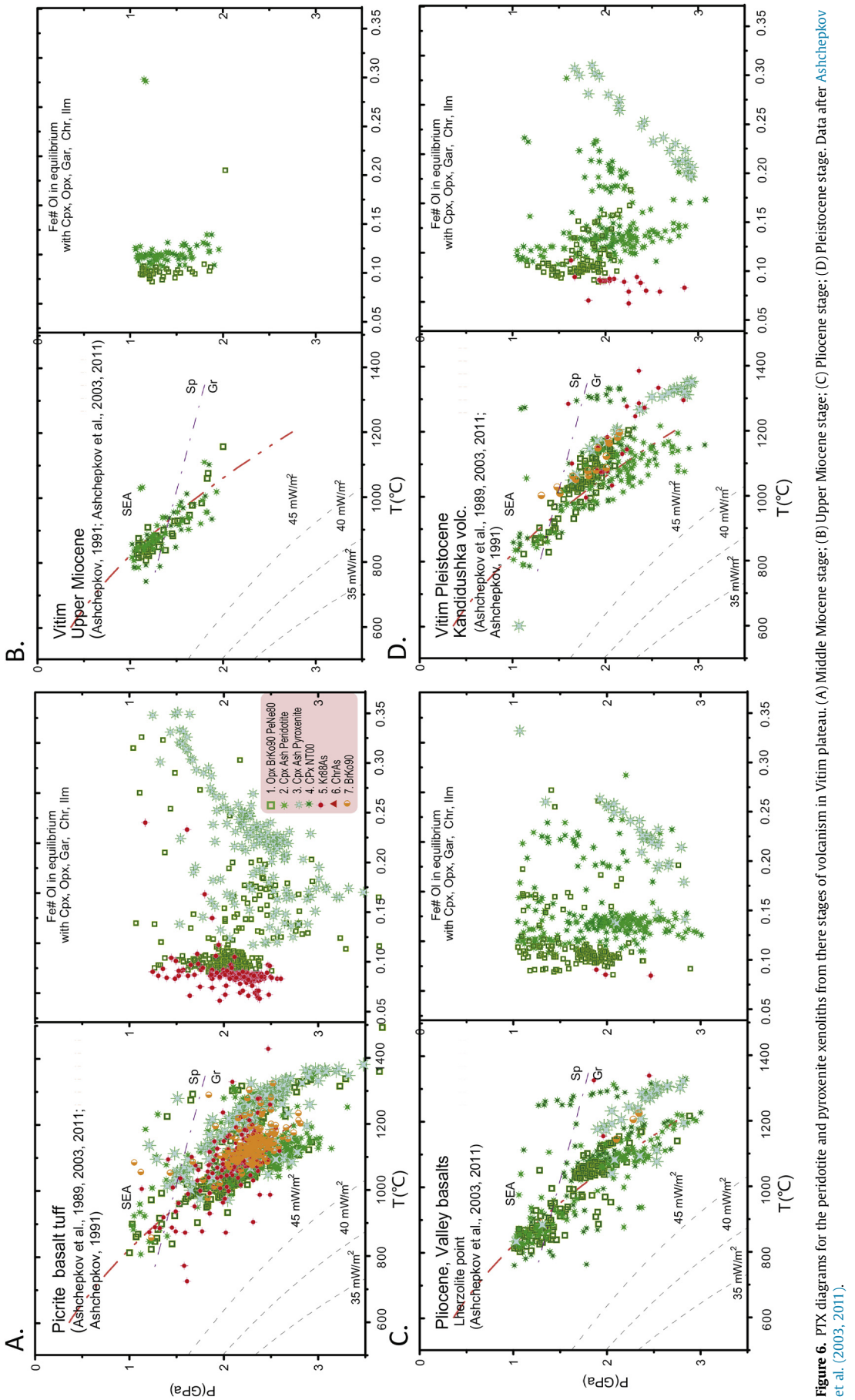

Figure 6. PTX diagrams for the peridotite and pyroxenite xenoliths from there stages of volcanism in Vitim plateau. (A) Middle Miocene stage; (B) Upper Miocene stage; (C) Pliocene stage; (D) Pleistocene stage. Data after Ashchepkov et al. (2003, 2011).

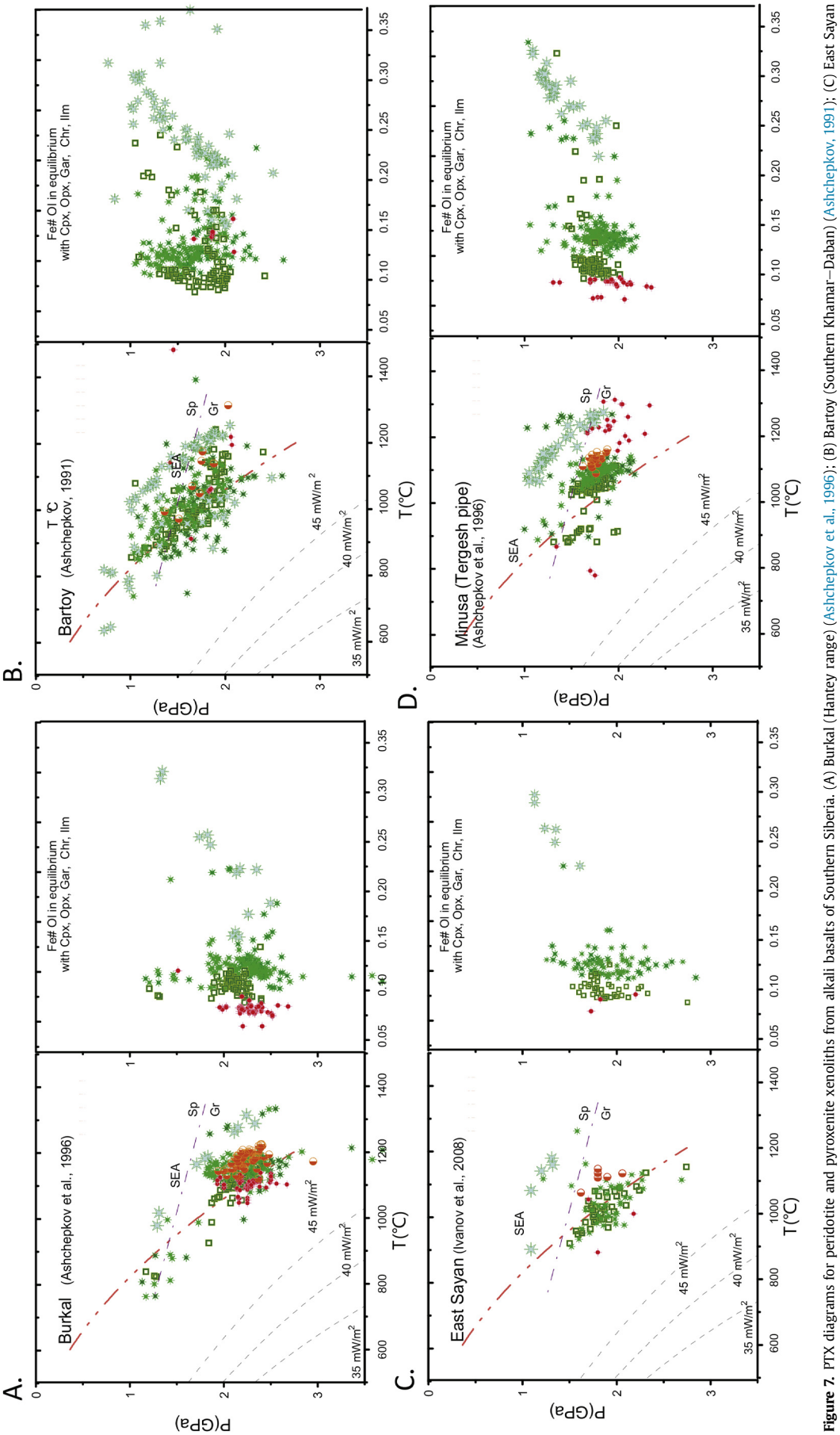

Figure 7. PTX diagrams for peridotite and pyroxenite xenoliths from alkali basalts of Southern Siberia. (A) Burkal (Hantey range) (Ashchepkov et al., 1996); (B) Bartoy (Southern Khamar–Daban) (Ashchepkov, 1991); (C) East Sayan (Ivanov et al., 2008); (D) Minusa (Tergesh pipe) (Ashchepkov et al., 1996).

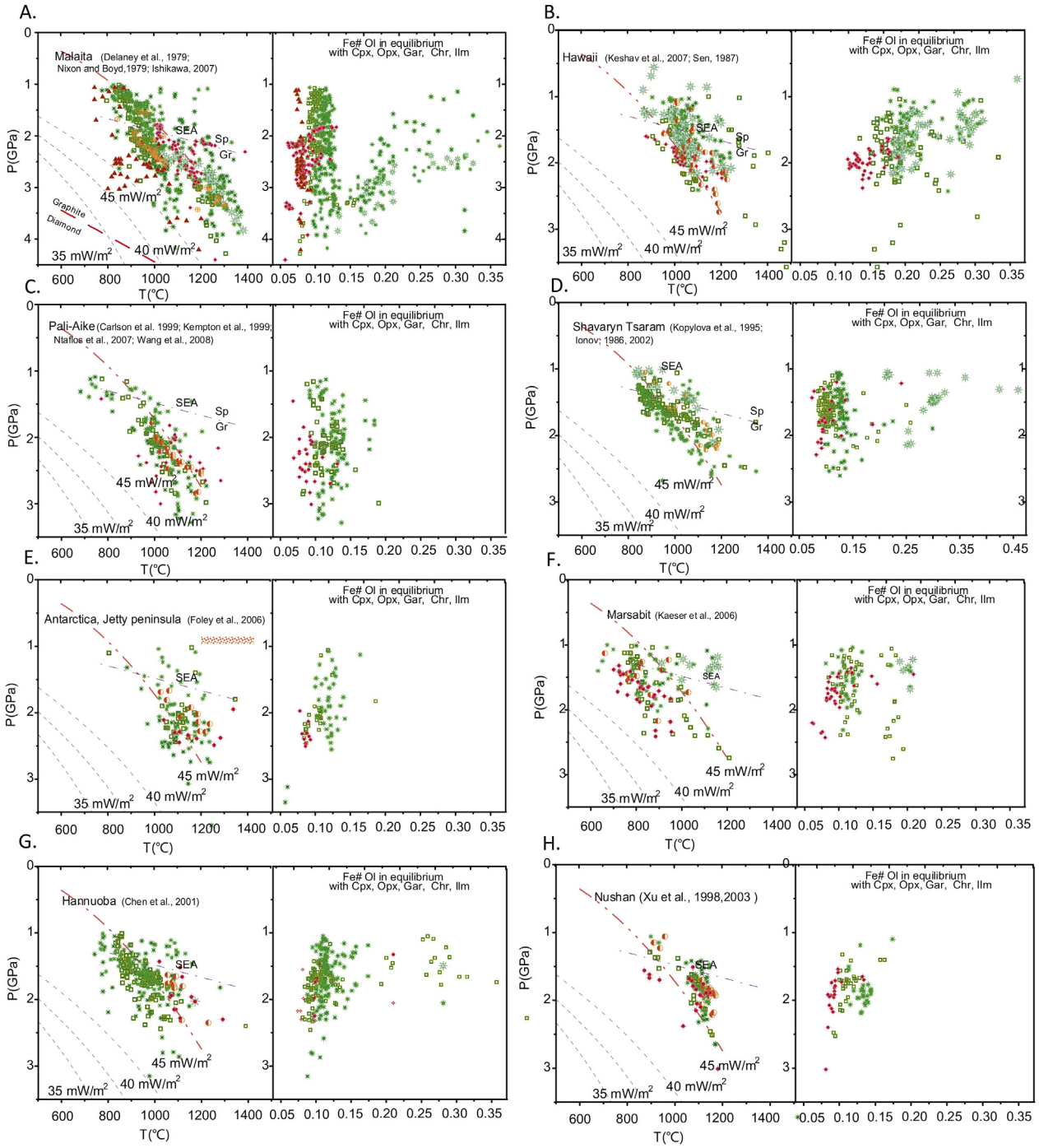

Figure 8. PTX diagrams for the peridotite and pyroxenite xenoliths from alkali basalts worldwide. (A) Malaita (Delaney et al., 1979; Nixon and Boyd, 1979; Ishikawa et al., 2004); (B) Hawaii (Sen, 1988; Sen and Leeman, 1991; Keshav et al., 2007); (C) Pali–Aike (Skewes and Stern, 1979; Bjerg et al., 2005; Ntaflos et al., 2007); (D) Mongolia (Shavaryn Tsaram) (Ionov, 1986, 2002; Kopylova et al., 1995); (E) Antarctica, Jetty peninsula (Foley et al., 2006); (F) Marsabit (Kaeser et al., 2006, 2007, 2009); (G) Hannuoba (China) (Chen et al., 2001); (H) Nushan (Xu et al., 1996, 2003).

rather high temperature conditions above the 90 mW/m^2 geotherm (Fig. 7D). Megacrystalline associations containing pyrope–almandine garnets also cover all the pressure interval of ~1.0–2.0 GPa.

5.3. Basalt localities with garnet peridotite xenoliths worldwide

Garnet-bearing associations in alkali basalts that can yield PT conditions using Gar–Opx thermobarometry are rare in the world. The universal Cpx barometry was also checked using the published associations from well-known localities.

Malaita. Xenoliths from alkali picrites from Malaita island yielded the pressure range from 4.0 to 1.2 GPa (Nixon and Boyd, 1979) and so construct a cold oceanic geotherm. Other rock types (Delaney et al., 1979; Ishikawa, 2007) yield a more detail PT diagram, showing that it consists of several branches. The prevailing high temperature branch found at the lithosphere base and upper part of mantle section refer to the 90 mW/m^2 geotherm but the

branch from 1.8 to 2.7 GPa relates to the 70 mW/m^2 geotherm (Fig. 8A). The associated megacrysts trace only the lower part of the HT (high temperature) branch from 4.0 to 2.5 GPa and reveal a trend typical for ascending magma with decreasing pressure and Mg$^{\#}$, but at ~2.5 GPa the differentiation was isobaric.

Hawaii. Xenoliths from alkali basalts in Hawaii are pyroxenites and Fe-rich peridotites (Sen, 1988; Keshav et al., 2007). They yield a rather complex geotherm consisting of branches showing the repeated intrusions of basaltic melts from a rather deep source because pyroxene temperatures reach >1400 °C. The deeper branch from 2.7 to 1.5 GPa corresponds to the more Mg-rich peridotites and pyroxenites probably formed from hybrid magmas while HT branches show a greater degree of heating and Fe$^{\#}$ reflecting progressive intrusions of differentiating basaltic melts (Fig. 8B).

Pali–Aike volcano in Patagonia (Skewes and Stern, 1979; Stern, 1991; Stern et al., 1999; Kempton et al., 1999; Bjerg et al., 2005; Ntaflos et al., 2007; Wang et al., 2008) erupted xenoliths in continental back-arc basalts. They differ from the other basaltic arc localities by lying on a relatively low temperature geotherm, slightly lower than the 90 mW/m^2 geotherm. Only the deeper part is slightly more heated at 2.5 GPa but again the mantle becomes cooler in its lower part. The fertilization and heating at this level is higher as is evident by the Fe$^{\#}$ for the Cpx and Opx. The megacrysts trend shows a gradual increase of Fe with decreasing pressures but also demonstrate an isobaric trend near the Moho (Fig. 8C).

Shavaryn–Tsaram volcano in Mongolia (Ionov, 1986, 2002; Kopylova and Genshaft, 1991; Kopylova et al., 1995) (Fig. 8D) contains garnet-bearing mantle xenoliths and also megacrystic pyropes and their intergrowths. In general xenoliths from this locality yield a geotherm located just on the 90 mW/m^2 conductive geotherm which is typical for xenoliths from alkali basalts. The megacrysts trend shows a gradual increase in Fe with decreasing pressures but it also demonstrates an isobaric trend near the Moho (Fig. 8D).

Antarctica. The xenoliths from the Jetty peninsular in Antarctica (Foley et al., 2006) include garnet-bearing peridotites. They yield higher temperatures and fall close to the 90 mW/m^2 conditions in the high pressure field at 2.5 GPa. The upper part of mantle column here composed mainly of pyroxenites (Fig. 8E).

Marsabit. In Northern Kenya, one locality contains abundant pyroxenitic xenoliths with garnets (Kaeser et al., 2006, 2007, 2009) with a rather wide compositional range and with higher Fe in the upper level just at the Moho. They demonstrate a cooling range from 90 to 60 mW/m^2 at 0.6 GPa and are possibly result from interaction of partial melts and basaltic magma with the lower crust (Fig. 8F). Authors suggest extensive decompression and cooling (970–1100 °C at 2.3–2.6 GPa to 700–800 °C at 0.5–1.0 GPa) during deformation.

Hannuoba locality in North Eastern China (Chen et al., 2001) (Fig. 8G) represents the typical situation for most other localities. Most of the spinel peridotite xenoliths trace the 90 mW/m^2 geotherm while the garnet-bearing ones are slightly hotter and, like in the Minusa depression, they are located above the Gar–Sp transition and are mainly pyroxenitic. They show rather wide dispersion in PT conditions (combined plot) as do the megacrysts (Fig. 8F). Hannuoba contains a high amount of garnet peridotites which yield higher temperature conditions than common spinel peridotites like those from the Kandidushka volcano in Vitim and probably represent the roof of the rising basaltic system and rock types affected by heating. Many pyroxenites are rather Fe-rich in this locality. The megacrysts there mainly relate to the lower magmatic chamber. The heating and elevated Fe$^{\#}$ of the Cpx in the uppermost part of mantle section probably reflect magma intrusion beneath the Moho (Fig. 8G).

Nushan, China. Described in detail by Xu et al. (1996, 2003), this locality contains spinel amphibole-bearing lherzolites, garnet pyroxenites and garnet lherzolites. The garnet-bearing varieties are rather high-temperature >90 mW/m^2 and are distributed in two pressure intervals. The Fe-rich pyroxenites correspond to 1 GPa at the Moho (Fig. 8H).

5.4. Kimberlitic xenoliths and reconstruction of the mantle sequences

The universal monomineral thermobarometers were applied to reconstruct the mantle sections beneath kimberlite pipes. They give a good opportunity for fast construction of geotherms and other diagrams.

5.4.1. Mantle xenoliths and heavy mineral separates from kimberlites

Thermobarometry for garnet (Ryan and Griffin, 1996; Ashchepkov et al., 2010, 2014) and clinopyroxenes (Nimis and Taylor, 2000; Ashchepkov et al., 2010, 2011) greatly helps in the construction of geotherms for the subcratonic lithospheric mantle (SCLM). In the diagram for xenoliths from the Udachnaya pipe (Fig. 9), the universal Cpx and Gar barometry were applied to different mantle lithologies: peridotites eclogites and pyroxenites. The calculated PT parameters for the peridotites show excellent coincidence with parameters determined by the Opx-based methods. The Cpx barometer of Ashchepkov et al. (2015) practically repeats all the PT groups and is even better than the method of Nimis and Taylor (2000) (Fig. 9A). The same is demonstrated by the method of Ashchepkov et al. (2015) which produces lower temperature geotherms in general. In this version, the monomineral methods for eclogites yield very high pressure and temperature range. Application of the method of Beyer et al. (2015) shows in general the same conditions but produced shallower pressure estimates (Fig. 9B). The calculations for pyroxenites (Kuligin, 1997; Pokhilenko et al., 1999) demonstrate good agreement of their position within the peridotitic mantle. Most relate to the high temperature branch of the geotherm. The garnet method again gives lower temperatures (Fig. 9D–F).

The new versions of the clinopyroxene and garnet barometry produced a reinterpretation of the mantle structure beneath the Mir pipe (Ashchepkov et al., 2010, 2014) and distinguished several groups of eclogites in the mantle section (Fig. 10A). General division of mantle eclogites to groups (Dawson, 1980) A (Mg-rich), B (common meta-basaltic) and C (high Fe–Na–Al) was completed by the addition of high Ca group (Spetsius et al., 2008; Viljoen et al., 2010). The geotherm for the Mir pipe (Fig. 10A) determined by Opx–Gar (Brey and Kohler, 1990) and garnet (Ashchepkov et al., 2010) thermobarometry is relatively low temperature near the lithosphere base, e.g. showing 1000 °C at 6.0 GPa. It cuts all conductive geotherms in the upper part and marks the advective PT path starting from the pyroxenite layer located at 3.5–4.0 GPa.

Most diamond-bearing eclogites (Sobolev et al., 1970; Beard et al., 1996) of Gr1 and Gr4 trace the diamond–graphite boundary (Kennedy and Kennedy, 1976) and yield rather high temperature conditions. The rather large group of points located above this may be explained by data after Day (2012) which gives this transition ~2.5 GPa higher. Mg-rich clinopyroxenes in group A (GrA) eclogites form a dense cluster (5–6 GPa) near the lithosphere base and are slightly hotter than xenoliths and garnet geotherm. The low-Cr varieties form a cloud in the P–Fe$^{\#}$ diagram in the 3.5–4.5 GPa pressure interval. For eclogites of groups B, C and D there are several trends of increasing Fe$^{\#}$ with pressure which characterize rising and differentiating melts. Ca-rich (GrD) eclogites are found within a rather wide pressure interval but mainly near the lithosphere asthenosphere boundary (LAB) and in the middle part of the mantle section. The points for the Fe- and Al-rich Group C form a cloud within the 3–5 GPa interval and in the level

Please cite this article in press as: Ashchepkov, I.V., et al., Monomineral universal clinopyroxene and garnet barometers for peridotitic, eclogitic and basaltic systems, Geoscience Frontiers (2016), http://dx.doi.org/10.1016/j.gsf.2016.06.012

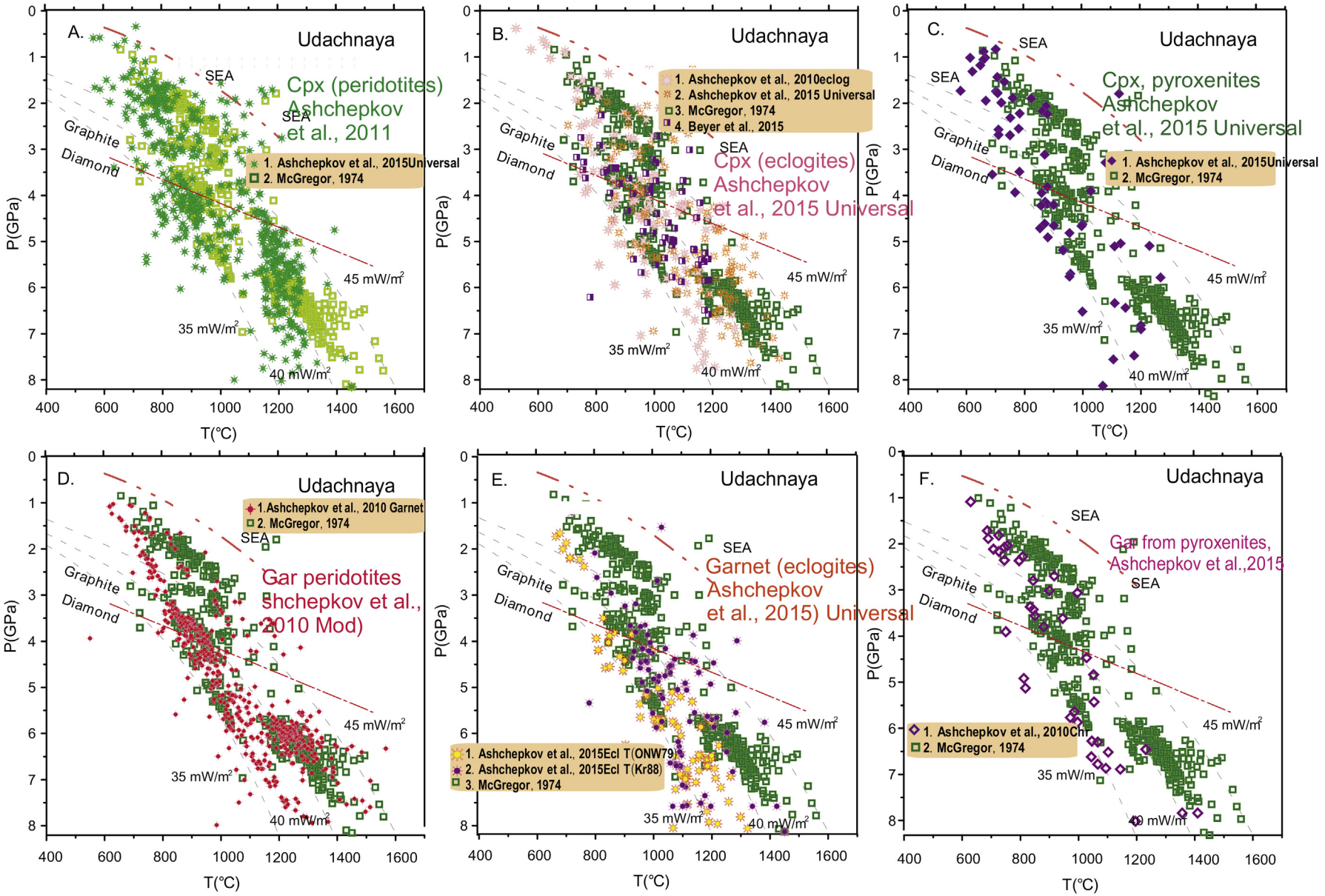

Figure 9. PT diagrams for mantle xenoliths from Udachnaya kimberlite pipe Yakutia. Comparison of the estimates with the Cpx and Garnet barometers with the Opx estimates T(°C) (Brey and Kohler, 1990) – P (GPa) (McGregor, 1974) for peridotites (A, D), eclogites (B, E), pyroxenites (C, F). Data: Sobolev et al. (1994), Kuligin et al. (1997), Pokhilenko et al. (1999), Malygina (2000), Pokhilenko (2006), Ashchepkov et al. (2013a,b) and references therein.

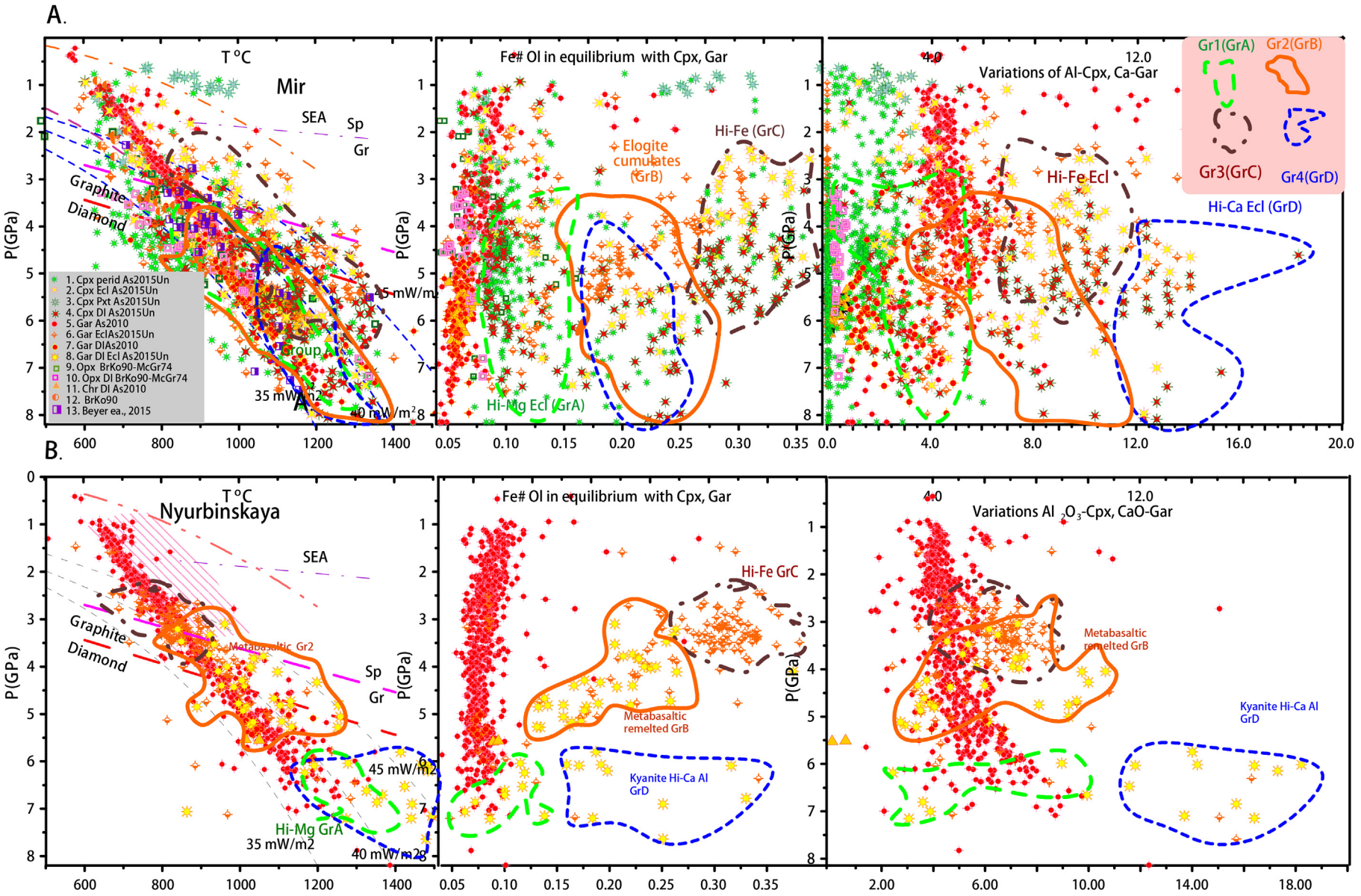

Figure 10. PTX diagram for xenoliths and minerals concentrates from: (A) Mir pipe and (B) Nyurbinskaya pipe. Symbols: 1. Cpx: T(°C) (Nimis and Taylor, 2000) Corr – P (GPa) (Ashchepkov et al., 2015, Un) for peridotes; 2. same for eclogites; 3. same for pyroxenites; 4. same for diamond inclusions; 5 garnet (monomineral): T(°C) (O'Neill and Wood, 1979; Monomin) – P (GPa) (Ashchepkov et al., 2010); 6. eclogitic garnets: T(°C) (O'Neill and Wood, 1979; Monomin) – P (GPa) (Ashchepkov et al., 2016) Ecl (This paper); 7. same for peridotitic diamond inclusions; 8. same for eclogitic diamond inclusions; 9. Opx: T(°C) (Brey and Kohler, 1990) – P (GPa) (McGregor, 1974); 10. same for diamond inclusions; 11. chromite for diamond inclusions: T(°C) (O'Neill and Wall, 1987) – P (GPa) (Ashchepkov et al., 2010); 12. Opx–Gar: T(°C) – P (GPa) (Brey and Kohler, 1990); 13. Cpx: T(°C) (Nimis and Taylor, 2000) Corr – P (GPa) (Beyer et al., 2015). The fields of the eclogite groups – see legend: Gr1(A)– dashed green line; Gr2(B)– dashed orange line; Gr3(C)– dotted-dashed brown line; Gr4(D)– dashed blue line. Position of conductive geotherms is after Pollack and Chapman (1977) and the graphite–diamond transition after Kennedy and Kennedy (1976); the line above is after Day (2012).

near 6 GPa. Omphacites in group C and group D (Ca-rich) eclogites occur on the relatively hot branches >45 mW/m^2, suggesting the influence of protokimberlites. Several low-Cr Gar and Cpx from group A and group B eclogites with relatively low Fe$^{\#}$ ~ 0.15 found in the lithosphere base may have crystallized from protokimberlites. Eclogites with low Fe$^{\#}$ ~ 0.11–0.15 found in the lithosphere base may have crystallized from protokimberlite magmas. The conditions determined with the Gar–Cpx method for the eclogitic diamond inclusions reveal their position near the Di–Gr transition over a wide temperature range.

The Nyurbinskaya pipe (Fig. 10B) contains a huge amount of eclogitic garnets of unusual Fe–Al-rich type (Spetsius, 2004; Spetsius et al., 2008) which are distributed in a wide pressure interval from the LAB to the Moho. Trends of P–Fe$^{\#}$ reveal an inflection near 3.5 GPa. The basaltic groups show increasing P–Fe$^{\#}$ from the SCLM base and descending from the top; they also reveal the inflection near this boundary. This boundary is also the upper limit for the pressure determined for the peridotitic diamond inclusions (Spetsius et al., 2008) and diamond-bearing eclogites. The latter form 4 groups from low-Fe to Fe-rich varieties, showing the increasing P–Fe$^{\#}$ trends from the LAB. The GrB groups reflect mostly low-T conditions and heating in the lower SCLM. Group 3–4 diamond-bearing eclogites reveal hotter conditions. Group 4 eclogites trace a nearly adiabatic trend in the upper part of the SCLM. Ca-rich (GrD) varieties are found from the LAB to the middle part of the mantle section. Some mantle sequences containing abundant

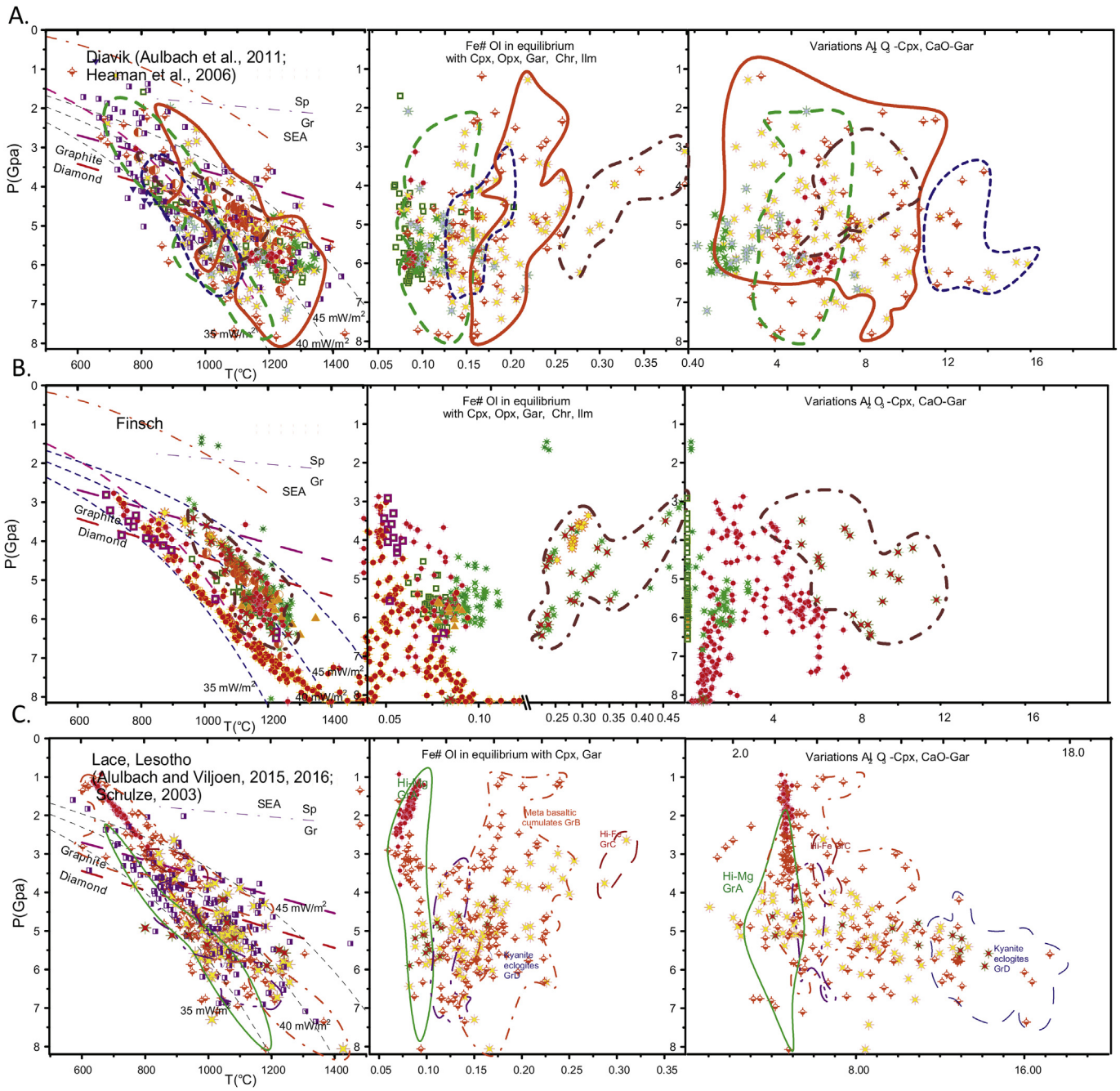

Figure 11. PTX diagram for xenoliths and minerals concentrates from (A) Diavik mine (Canada); (B) Finsch pipe (South Africa); (C) Lace pipe (Lesotho) (Aulbach and Viljoen, 2016; Aulbach et al., 2016). Symbols are same as Fig. 10.

Please cite this article in press as: Ashchepkov, I.V., et al., Monomineral universal clinopyroxene and garnet barometers for peridotitic, eclogitic and basaltic systems, Geoscience Frontiers (2016), http://dx.doi.org/10.1016/j.gsf.2016.06.012

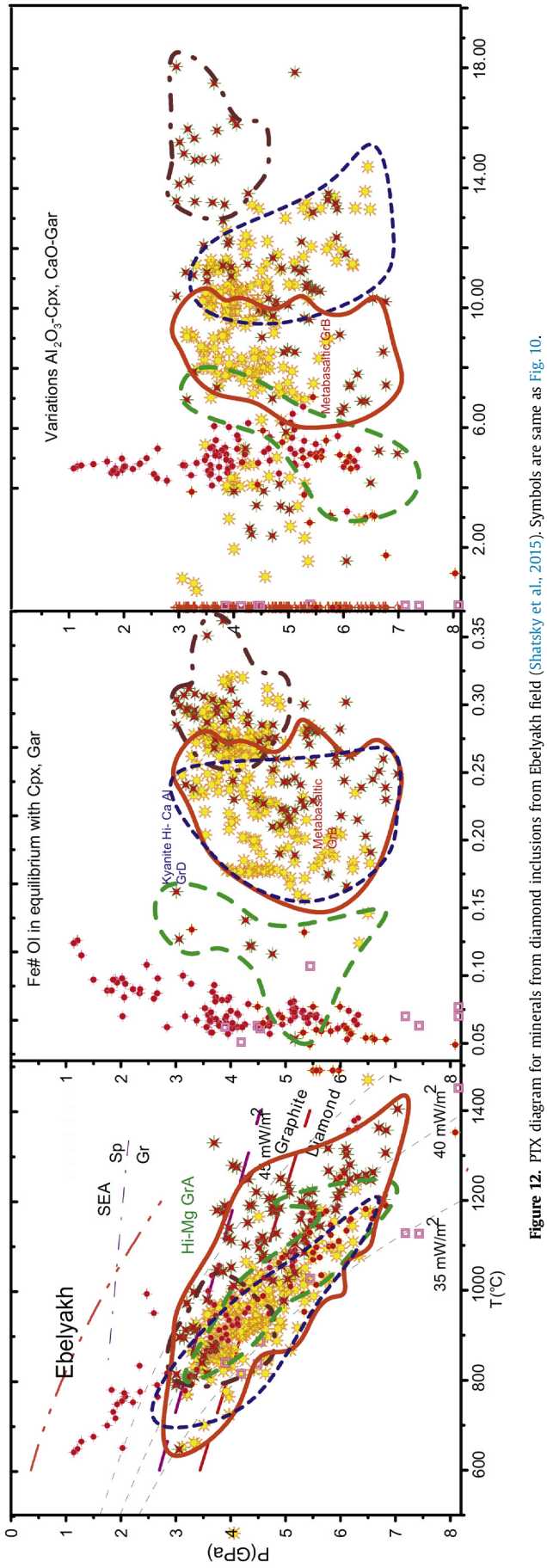

Figure 12. PTX diagram for minerals from diamond inclusions from Ebelyakh field (Shatsky et al., 2015). Symbols are same as Fig. 10.

Fe-rich eclogites like those beneath the Nyurbinskaya pipe (Spetsius, 2004; Spetsius et al., 2008; Riches et al., 2010) possibly contain subducted material which was not extensively melted. Such an unusual construction of mantle section suggests growth of the craton keel according to the stacked slab model (Griffin et al., 2003) with the repetition of similar sequences but the presence of the Ca-rich associations mainly in the lower SCLM allows us to suggest other explanations (Pearson and Wittig, 2014).

Slave Craton, Canada. Large collections of eclogite xenoliths from the Diavik mine (Aulbach et al., 2007, 2008, 2011; Cartigny et al., 2009) provide the possibility to compare the structure of mantle lithosphere beneath the central part of Slave craton with that beneath the Jericho pipe in the North Slave (Heaman et al., 2006; Kopylova et al., 2009). The GrC eclogites including diamond-bearing varieties are found mainly to the middle part of the mantle section The GrB and GrA show a rather wide pressure interval. Those from the upper part of the mantle column yield a heated geotherm commonly corresponding to the pyroxenites. Typical pyroxenites yield low temperature conditions and occur in the 4–6 GPa pressure interval. The GrA eclogites which mainly trace the lower horizons of the mantle lithosphere are cooler than other groups (Fig. 11A). The pressure range for the eclogites determined by the method of Beyer et al. (2015) in combination with the Krogh (1988) thermometer shows similar variations as those determined by the method of Ashchepkov et al. (2015) but with slightly lower temperatures.

Southern Africa. Well studied mantle xenoliths (Gibson et al., 2008; Lazarov et al., 2009), xenocrysts and diamond inclusions (Gurney et al., 1979; Shirey et al., 2001; Tsai et al., 1979; Appleyard et al., 2004; Viljoen et al., 2010) from the Finsch pipe already yielded PTX diagrams (Ashchepkov et al., 2012). In this version of the diagram, we re-calculated the PT conditions for the omphacites which are the most Fe-rich, and also the PT conditions for relatively Fe-rich eclogitic garnets which gave conditions very close to those calculated from the clinopyroxenes (Fig. 11B). Xenoliths from the Lace pipe in Lesotho (Aulbach and Viljoen, 2016; Aulbach et al., 2016) reveal a wide PT range and heating at the LAB. The PT conditions of the diamond kyanite eclogites are mostly close to the graphite–diamond boundary (Fig. 11C).

5.4.2. Diamond inclusions

The universal barometers are very useful for calculations of the PT values of diamond inclusions (Logvinova et al., 2005). In previous publications (Ashchepkov et al., 2010, 2012, 2013a,b, 2014, 2015), we calculated PT conditions for many worldwide kimberlite localities. Now it is possible to add the results for pyrope almandine garnets from eclogites.

Eclogite thermobarometry may be very useful for reconstruction of mantle sections using only inclusions in diamond from placers such as those from the Ebelyakh field (Fig. 12) (Shatsky et al., 2015) of late Devonian age (Afanasyev et al., 2009). Garnets and clinopyroxenes from this locality belong mainly to eclogitic groups 2 (B) and 4 (Ca-Al rich), but, among the diamond inclusions, Ca-rich garnets are frequent and belong mainly to the lower part of mantle section. The basaltic groups show three clusters according to their Fe# values and reveal at least three ascending Fe# trends from the LAB to the Moho. Clinopyroxenes from GrC show an increase of Al to the LAB (Fig. 6A). The GrD clinopyroxenes show both Fe- and Al-enrichment. Splitting of the trend near 3–3.5 GPa is visible for the most Fe-rich eclogites. The Ca-rich GrD and pyrope diamond inclusions also trace this level. The lowermost group of eclogitic diamond inclusions shows rather low-T conditions close to those calculated for the peridotitic garnets and clinopyroxenes. But those from the middle part of SCLM demonstrate rather high-T conditions corresponding to the advective mantle geotherm. The

eclogitic diamond inclusions from the deepest parts of the SCLM yield rather low-T conditions close to those calculated for peridotitic garnets and orthopyroxenes. But diamond inclusions from the Ca-rich group 3 and group 4 from the middle part of the SCLM demonstrate rather high-T conditions, corresponding to the advective mantle geotherm.

6. Conclusions

(1) Precision of universal clinopyroxene barometer is comparable with that of the reliable published methods;
(2) Mantle sections for xenoliths in alkali basalts generally fall on the 90 mW/m^2 geotherm and slightly lower in arc settings;
(3) In mantle sections beneath kimberlite pipes, the PT conditions for all rock groups generally coincide;
(4) Eclogites and mantle inclusions often show colder ancient thermal conditions of thick lithosphere.

Acknowledgements

The data for the kimberlite peridotite inclusions from Yakutian kimberlite pipes were obtained during performing the projects with the ALROSA Company and the works on the research projects RFBR. Many thanks contribute to Dr. Nick Roberts for the final corrections of the manuscript. The work was supported by RBRF (Grant Nos. 11-05-00060a, 16-05-00860a).

Appendix. Application thermobarometric methods in PT program

Original monomineral thermobarometers for mantle peridotites for clinopyroxene, garnet, chromite and ilmenites for the mantle peridotites were statistically calibrated on the PT estimates for mantle peridotites (Ashchepkov et al., 2010) were combined in the original program written in FORTRAN (Ashchepkov et al., 2013a,b) are assembled with the most reliable methods of mineral thermometers (45) and barometers (36) and oxybarometers (5), including original monomineral and methods (Ashchepkov, 2003; Ashchepkov et al., 2010, 2011) for mantle peridotites based on the compositions of on clinopyroxene, garnet, chromite and ilmenite. Program reads the text files, which converted from Excel. Original data includes standard silicate compositions for 12 components in standard order. The text file includes 15 columns of 8 symbols. The first is file name which is the same for all the minerals in the association. The second is indicator symbol for phases: E—enstatite, D—diopside, O—olivine, S-spinel, G—garnet, I—ilmenite, A—amphibole, F—phlogopite, P—plagioclase, L—liquid, R—bulk rock. Then follow oxides: SiO_2, TiO_2, Al_2O_3, Cr_2O_3, FeO, MnO, MgO, CaO, Na_2O, K_2O, NiO, V_2O_3 written with 2 or 3 decimals. The last column may contain description of the mineral or association up to 64 symbols. Monomineral methods use calculated values for Fe$^{\#}$Ol or Fe$^{\#}$Cpx and also Fe^{3+} and other characteristic parameters. The input from console includes file name (8 symbols) (A8), then amount of PT pairs of numbers thermometers and barometers (2I2) and one for $f(O_2)$ method. Program allows input of the iteration numbers (25 by default). It is possible also to put fixed values of T and P (default 1000 °C and 40 GPa).

The program reads mineral compositions detecting them by mineral indexes with the name of the association are the same and start the estimations of PT values when read different names. They are going to the dispatcher points sending to the thermometers and barometers according to the input numbers. It performs calculations for each pair until the difference of the temperatures is higher 1° or less than iteration number made then goes to next pair. The values of calculates pairs are writing in the matrix. It begins new line and circle of calculations when the new name of probe appears.

The results of the calculations of pairs (to 15) PT of the parameters in any combination are writing in the matrix of data in the CSV format together with the compositions of minerals or their formula coefficients. The calculated Fe$^{\#}$Ol for coexisting olivine for each mineral are written also as well as Cr$^{\#}$ and Fe^{3+} for comites and Fe^{3+} for Cpx. The description is writing before the results of the calculations. The CSV files are easily converting to Excel or Grapher and Surfer or may be used for the statistical programs.

Special variety of programs works with the data files of the experimental PT values and data of the minerals in runs (see Supplementary file 5) reading PT parameters and writing them together with the calculated values and compositions of the minerals. This allows to make the correlations of compositions of minerals and PT values of the experimental runs and results of the approximations and to find the difference between the P and T difference and their dependence from mineral, liquid or even starting rock compositions.

Corrected equation of the Cpx barometer published in Ashchepkov et al. (2011) is listed below:

$$AlCr = (Al - 0.01) \times ((T°K - 600)/650)^{0.75} + Cr \times (T°K - 100)/900 + (4 \times Ti - 0.0125)/(T°K - 801) \times 650 + (Fe - 0.23) \times (T°K - 700)/21000;$$

$$K_D = Na/AlCr \times MgO/CaO$$

$$P = 0.028 \times K_D \times T°K/(1 + 2.05 \times Fe - 1.15 \times Fe \times (T°K - 600)/1200) - \ln(1273/T°K) \times 40 \times (-Al + 7 \times Na - 15 \times Ti + 10 \times Cr + Mg/4) + 7.5 \times Si + 50 \times (Na + 0.10 \times Al - 2 \times Ti + 0.05 \times Mg - 0.2 \times Ca - 0.75 \times Na/Ca)$$

Appendix A. Supplementary data

Supplementary data related to this article can be found at http://dx.doi.org/10.1016/j.gsf.2016.06.012.

References

Afanasyev, V.P., Agashev, A.M., Orihashi, Y., Pokhilenko, N.P., Sobolev, N.V., 2009. Paleozoic U–Pb age of rutile inclusions in diamonds of the V–VII variety from placers of the Northeast Siberian platform. Doklady Earth Sciences 428, 1151–1155.

Appleyard, C.M., Viljoen, K.S., Dobbe, R., 2004. A study of eclogitic diamonds and their inclusions from the Finsch kimberlite pipe, South Africa. Lithos 77, 317–332.

Ashchepkov, I.V., 1991. Mantle Xenoliths of the Baikal Rift. Nauka, Novosibirsk, 160 p (in Russian).

Ashchepkov, I.V., 2002. Empirical clinopyroxene thermobarometers for mantle rocks based on the diopside-jadeite exchange. Doklady Earth Sciences 382, 366–370.

Ashchepkov, I.V., 2003. More Precise Equation of the Jd- En barometer. Herald of the Department of Earth Sciences RAS" N1 (21) 2003. http://www.scgis.ru/russian/cp1251/h_dgggms/1-2003/informbul-1_2003/term-7e.pdf.

Ashchepkov, I.V., 2006. Empirical garnet thermobarometer for mantle peridotites. Russian Geology and Geophysics 47, 1071–1085.

Ashchepkov, I.V., 2011. Program of the mantle thermometers and barometers: usage for reconstructions and calibration of PT methods. Vestnik Otdelenia nauk o Zemle RAN 3, NZ6008.

Ashchepkov, I.V., Ionov, D.A., 1999. Metasomatic mantle beneath Bartoy volcanoes – the ancient continental margin or the recent interaction with the hydrous plume melts? Ofioliti 24, 51–52.

Ashchepkov, I.V., Dobretsov, N.L., Kalmanovich, M.A., 1989. Garnet peridotite xenoliths from alkali picritoid and basanitoid of the Vitim Plateau. Doklady USSR Academy of Sciences, Earth Science Section 302, 156–159.

Ashchepkov, I.V., Kepezhinskas, V.V., Malkovets, V.G., Ovchinnikov, Y.I., 1995. Mantle Xenoliths from the Meso-Cenozoic Volcanic Pipes of Khakassia. Field guide book: 6th Int. Kimberlite Conf. Novosibirsk, 39 p.

Ashchepkov, I.V., Litasov, Yu.D., Litasov, K.D., 1996. Xenoliths of garnet xenoliths from nephelinites, the Khentey ridge (Southern Transbaikalia): evidence of the mantle diapir ascend. Russian Geology and Geophysics 37, 121–137.

Ashchepkov, I.V., Andre, L., 2002. Differentiation of the mantle melts: an example of the pyroxenite xenoliths from picrite basalts Vitim plateau. Russian Geology and Geophysics 43 (4), 343–363.

Ashchepkov, I.V., Travin, S.V., Saprykin, A.I., Andre, L., Gerasimov, P.A., Khmel'nikova, O.S., 2003. Age of xenolith-bearing basalts and mantle evolution in the Baikal rift zone. Russian Geology and Geophysics 44, 1160–1188.

Ashchepkov, I.V., Pokhilenko, N.P., Vladykin, N.V., Logvinova, A.M., Kostrovitsky, S.I., Afanasiev, V.P., Pokhilenko, L.N., Kuligin, S.S., Malygina, L.V., Alymova, N.V., Khmelnikova, O.S., Palessky, S.V., Nikolaeva, I.V., Karpenko, M.A., Stegnitsky, Y.B., 2010. Structure and evolution of the lithospheric mantle beneath Siberian craton, thermobarometric study. Tectonophysics 485, 17–41.

Ashchepkov, I.V., André, L., Downes, H., Belyatsky, B.A., 2011. Pyroxenites and megacrysts from Vitim Picrite-basalts Russia: polybaric fractionation of rising melts in the mantle? Journal of Asian Earth Sciences 42, 14–37.

Ashchepkov, I.V., Rotman, A.Y., Somov, S.V., Afanasiev, V.P., Downes, H., Logvinova, A.M., Nossyko, S., Shimupi, J., Palessky, S.V., Khmelnikova, O.S., Vladykin, N.V., 2012. Composition and thermal structure of the lithospheric mantle beneath kimberlite pipes from the Catoca cluster, Angola. Tectonophysics 530–531, 128–151.

Ashchepkov, I.V., Vladykin, N.V., Ntaflos, T., Downes, H., Mitchel, R., Smelov, A.P., Rotman, A.Ya., Stegnitsky, Yu., Smarov, G.P., Makovchuk, I.V., Nigmatulina, E.N., Khmelnikova, O.S., 2013a. Regularities of the mantle lithosphere structure and formation beneath Siberian craton in comparison with other cratons. Gondwana Research 23, 4–24.

Ashchepkov, I.V., Ntaflos, T., Kuligin, S.S., Malygina, E.V., Agashev, A.M., Logvinova, A.M., Mityukhin, S.I., Alymova, N.V., Vladykin, N.V., Palessky, S.V., Khmelnikova, O.S., 2013b. Deep-seated xenoliths from the brown breccia of the Udachnaya pipe, Siberia. In: Pearson, D.G., et al. (Eds.), Proceedings of 10th International Kimberlite Conference, vol. 1. Springer India, New Delhi, pp. 59–74.

Ashchepkov, I.V., Vladykin, N.N., Ntaflos, T., Kostrovitsky, S.I., Prokopiev, S.A., Downes, H., Smelov, A.P., Agashev, A.M., Logvinova, A.M., Kuligin, S.S., Tychkov, N.S., Salikhov, R.F., Stegnitsky, Yu.B., Alymova, N.V., Vavilova, M.A., Minin, V.A., Babushkina, S.A., Ovchinnikov, Yu.I., Karpenko, M.A., Tolstov, A.V., Shmarov, G.P., 2014. Layering of the lithospheric mantle beneath the Siberian Craton: modeling using thermobarometry of mantle xenolith and xenocrysts. Tectonophysics 634, 55–75.

Ashchepkov, I.V., Logvinova, A.M., Spetsius, Z.V., Stegnitsky, Yu.B., 2015. Monomineral Mantle Eclogite CPx and Garnet Thermobarometry. Goldschmidt Conference Abstracts, p. 126.

Ashchepkov, I.V., Ntaflos, T., Spetsius, Z.V., Salikhov, R.F., Downes, H., 2016. Interaction between protokimberlite melts and mantle lithosphere: evidence from mantle xenoliths from the Dalnyaya kimberlite pipe, Yakutia (Russia). Geoscience Frontiers. http://dx.doi.org/10.1016/j.gsf.2016.05.008 (in press).

Aulbach, S., Gerdes, A., Viljoen, K.S., 2016. Formation of diamondiferous kyanite–eclogite in a subduction mélange. Geochimica et Cosmochimica Acta 179, 156–176.

Aulbach, S., Viljoen, K.S., 2016. Eclogite xenoliths from the Lace kimberlite, Kaapvaal craton: from convecting mantle source to palaeo-ocean floor and back. Earth and Planetary Science Letters 431, 274–286.

Aulbach, S., Pearson, N.J., O'Reilly, S.Y., Doyle, B.J., 2007. Origins of xenolithic eclogites and pyroxenites from the Central Slave Craton, Canada. Journal of Petrology 48, 1843–1873.

Aulbach, S., Stachel, T., Heaman, L.M., Carlson, J.A., 2011. Microxenoliths from the Slave craton: archives of diamond formation along fluid conduits. Lithos 126, 419–434.

Aulbach, S., O'Reilly, S.Y., Griffin, W.L., Pearson, N.J., 2008. Subcontinental lithospheric mantle origin of high niobium/tantalum ratios in eclogites. Nature Geoscience 1, 468–472.

Beard, B.L., Fraracci, K.N., Taylor, L.A., Snyder, G.A., Clayton, R.N., Mayeda, T.K., Sobolev, N.V., 1996. Petrography and geochemistry of eclogites from the Mir kimberlite, Yakutia, Russia. Contributions to Mineralogy and Petrology 125, 293–310.

Bertrand, P., Mercier, J.C.C., 1985. The mutual solubility of coexisting ortho- and clinopyroxene: toward the absolute geothermometer for the natural system? Earth and Planetary Science Letters 76, 122–152.

Beyer, C., Frost, D.J., Miyajima, N., 2015. Experimental calibration of a garnet–clinopyroxene geobarometer for mantle eclogites. Contributions to Mineralogy and Petrology 169, 18–21.

Bjerg, E.A., Ntaflos, T., Kurat, G., Dobosi, G., Labudia, C.H., 2005. The upper mantle beneath Patagonia, Argentina, documented by xenoliths from alkali basalts. Journal of South American Earth Sciences 18, 125–145.

Bobrov, A.V., Dymshits, A.M., Litvin, Yu A., 2009. Conditions of magmatic crystallization of Na-bearing majoritic garnets in the earth mantle: evidence from experimental and natural data. Geochemistry International 47, 951–965.

Brey, G.P., Kohler, T., 1990. Geothermobarometry in four-phase lherzolites. II. New thermobarometers, and practical assessment of existing thermobarometers. Journal of Petrology 31, 1353–1378.

Brey, G.P., Nickel, K.G., Kogarko, L., 1986. Garnet–pyroxene equilibria in the system $CaO–MgO–Al_2O_3–SiO_2$ (CMAS): prospects for simplified ('T-independent') lherzolite barometry and an eclogite-barometer. Contributions to Mineralogy and Petrology 92, 448–455.

Bulatov, V.K., Brey, G.P., Girnis, A.V., Gerdes, A., Höfer, H.E., 2014. Carbonated sediment–peridotite interaction and melting at 7.5–12 Gpa. Lithos 200–201, 368–385.

Cartigny, P., Farquhar, J., Thomassot, E., Harris, J.W., Wing, B., Masterson, A., McKeegan, K., Stachel, T., 2009. A mantle origin for Paleoarchean peridotitic diamonds from the Panda kimberlite, Slave Craton: evidence from ^{13}C-, ^{15}N- and $^{33,34}S$-stable isotope systematics. Lithos 112, 852–864.

Chen, S.H., O'Reilly, S.Y., Zhou, X.H., Griffin, W.L., Zhang, G.H., Sun, M., Feng, J.L., Zhang, M., 2001. Thermal and petrological structure of the lithosphere beneath Hannuoba, Sino–Korean craton, China: evidence from xenoliths. Lithos 56, 267–301.

Dawson, J.B., 1980. Kimberlites and their Xenoliths. Springer-Verlag, Berlin, 252 p.

Day, H.W., 2012. A revised diamond–graphite transition curve. American Mineralogist 97, 52–62.

Delaney, J.S., Smith, J.V., Nixon, P.H., 1979. Model for upper mantle below Malaita, Solomon Islands, deduced from chemistry of lherzolite and megacryst minerals. Contributions to Mineralogy and Petrology 70, 209–218.

Doroshev, A.M., Brey, G.P., Girnis, A.V., Turkin, A.I., Kogarko, L.N., 1997. Pyrope-knorringite series in the Earth's mantle: an experimental study in the system $MgO–Al_2O_3–SiO_2–Cr_2O_3$. Russian Geology and Geophysics 38, 523–545.

Ellis, D.J., Green, D.H., 1979. An experimental study of the effect of Ca upon garnet–clinopyroxene Fe–Mg exchange equilibria. Contributions to Mineralogy and Petrology 71, 13–22.

Finnerty, A.A., Boyd, F.R., 1987. Thermobarometry for garnet peridotite xenoliths: a basis for upper mantle stratigraphy. In: Nixon, P.H. (Ed.), Mantle Xenoliths. Wiley, Chichester, pp. 381–402.

Foley, S.F., Andronikov, A.V., Jacob, D.E., Melzer, S., 2006. Evidence from Antarctic mantle peridotite xenoliths for changes in mineralogy, geochemistry and geothermal gradients beneath a developing rift. Geochimica et Cosmochimica Acta 70, 3096–3120.

Gibson, S., Malarkey, J., Day, J.A., 2008. Melt depletion and enrichment beneath the Western Kaapvaal craton: evidence from Finsch peridotite xenoliths. Journal of Petrology 49, 1915–1929.

Girnis, A.V., Bulatov, V.K., Brey, G.P., Gerdes, A., Höfer, H.E., 2013. Trace element partitioning between mantle minerals and silico-carbonate melts at 6–12 GPa and applications to mantle metasomatism and kimberlite genesis. Lithos 160–161, 183–200.

Glaser, S.M., Foley, S.F., Gunther, D., 1999. Trace element compositions of minerals in garnet and spinel peridotite xenoliths from the Vitim volcanic field, Transbaikalia, eastern Siberia. Lithos 48, 263–285.

Goncharov, A.G., Ionov, D.A., Doucet, L.S., Pokhilenko, L.N., 2012. Thermal state, oxygen fugacity and C–O–H fluid speciation in cratonic lithospheric mantle: new data on peridotite xenoliths from the Udachnaya kimberlite, Siberia. Earth and Planetary Science Letters 357–358, 99–110.

Griffin, W.L., O'Reilly, S.Y., Abe, N., Aulbach, S., Davies, R.M., Pearson, N.J., Doyle, B.J., Kivi, K., 2003. The origin and evolution of Archean lithospheric mantle. Precambrian Research 127, 19–41.

Grütter, H.S., Latti, D., Menzies, A., 2006. Cr-saturation arrays in concentrate garnet compositions from kimberlite and their use in mantle barometry. Journal of Petrology 47, 801–820.

Gurney, J.J., Jakob, W.R.O., Dawson, J.B., 1979. Megacrysts from the Monastery kimberlite pipe, South Africa. In: Boyd, F.R., Meyer, H.O.A. (Eds.), Proceedings of the Second International Kimberlite Conference, American Geophysical Union: The Mantle Sample: Inclusions in Kimberlites and Other Volcanics, vol. 2, pp. 227–243.

Harley, S.L., 1984. The solubility of alumina in orthopyroxene coexisting with garnet in $FeO–MgO–Al_2O_3–SiO_2$ and $CaO–FeO–MgO–Al_2O_3–SiO_2$. Journal of Petrology 25, 665–696.

Heaman, L., Creaser, R.A., Cookenboo, H., Chacko, T., 2006. Multi-stage modification of the Northern slave mantle lithosphere: evidence from zircon- and diamond-bearing eclogite xenoliths entrained in Jericho kimberlite, Canada. Journal of Petrology 47, 821–858.

Ionov, D.A., 1986. Spinel peridotite xenoliths from the Shavaryn–Tsaram Volcano, northern Mongolia: petrography, major element chemistry and mineralogy. Geologicky Sbornik 37 (6), 681–692.

Ionov, D., 2002. Mantle structure and rifting processes in the Baikal–Mongolia region: geophysical data and evidence from xenoliths in volcanic rocks. Tectonophysics 351, 41–60.

Ionov, D.A., Ashchepkov, I., Jagoutz, E., 2005. The provenance of fertile off-craton lithospheric mantle: Sr–Nd isotope and chemical composition of garnet and spinel peridotite xenoliths from Vitim, Siberia. Chemical Geology 217, 41–75.

Ionov, D.A., Doucet, L.S., Ashchepkov, I.V., 2010. Composition of the lithospheric mantle in the Siberian craton: new constraints from fresh peridotites in the Udachnaya-East kimberlite. Journal of Petrology 51, 2177–2210.

Ishikawa, A., Maruyama, S., Komiya, T., 2004. Layered lithospheric mantle beneath the Ontong Java plateau: implications from xenoliths in beneath the Ontong Java plateau: implications from xenoliths in Alnoite, Malaita, Solomon Islands. Journal of Petrology 45, 2011–2044.

Ishikawa, A., Kuritani, T., Makishima, A., Nakamura, E., 2007. Ancient recycled crust beneath the Ontong Java plateau: isotopic evidence from the garnet clinopyroxenite xenoliths, Malaita. Solomon Islands Earth and Planetary Science Letters 259, 134–148.

Ivanov, A.V., Palesskii, S.V., Demonterova, E.I., Nikolaeva, I.V., Ashchepkov, I.V., Rasskazov, S.V., 2008. Platinum-group elements and rhenium in mantle xenoliths from the East Sayan volcanic field (Siberia, Russia): evaluation of melt extraction and refertilization processes in lithospheric mantle of the Tuva–Mongolian massif. Terra Nova 20, 504–511.

Johnson, J.S., Gibson, S.A., Thompson, R.N., Nowell, G.M., 2005. Volcanism in the Vitim volcanic field, Siberia: geochemical evidence for a mantle plume beneath the Baikal rift zone. Journal of Petrology 46, 1309–1344.

Please cite this article in press as: Ashchepkov, I.V., et al., Monomineral universal clinopyroxene and garnet barometers for peridotitic, eclogitic and basaltic systems, Geoscience Frontiers (2016), http://dx.doi.org/10.1016/j.gsf.2016.06.012

Kaeser, B., Kalt, A., Pettke, T., 2006. Evolution of the lithospheric mantle beneath the Marsabit volcanic field (Northern Kenya): constraints from textural, P–T and geochemical studies on xenoliths. Journal of Petrology 47, 2149–2184.

Kaeser, B., Kalt, A., Pettke, T., 2007. Crystallization and breakdown of metasomatic phases in graphite-bearing peridotite xenoliths from Marsabit (Kenya). Journal of Petrology 48, 1725–1760.

Kaeser, B., Olker, B., Kalt, A., Pettke, T., 2009. Pyroxenite xenoliths from Marsabit (Northern Kenya): evidence for different magmatic events in the lithospheric mantle and interaction between peridotite and pyroxenite. Contributions to Mineralogy and Petrology 157, 453–472.

Kempton, P.D., Lopez-Escobar, L., Hawkesworth, C.J., Pearson, D.G., Ware, A.J., 1999. Spinel ± garnet lherzolite xenoliths from Pali Aike: Part 1. Petrology, mineral chemistry and geothermobarometry. In: Gurney, J.J., Gurney, J.L., Pascoe, M.D., Richardson, S.H. (Eds.), The J.B., Dawson Volume, Proceedings of the International Kimberlite Conference 7, vol. 1, pp. 403–414.

Kennedy, C.S., Kennedy, G.C., 1976. The equilibrium boundary between graphite and diamond. Journal of Geophysical Research 8, 12467–12470.

Keshav, S., Sen, G., Presnall, D.C., 2007. Garnet-bearing xenoliths from Salt lake crater, Oahu, Hawaii: high-pressure fractional crystallization in the oceanic mantle. Journal of Petrology 48, 681–1724.

Kiseeva, E.S., Yaxley, G.M., Hermann, J., Litasov, K.D., Rosenthal, A., Kamenetsky, V.S., 2012. An experimental study of carbonated eclogite at 3·5–5·5 GP – implications for silicate and carbonate metasomatism in the cratonic mantle. Journal of Petrology 53, 727–759.

Kopylova, M.G., Genshaft, S., 1991. Petrology of Garnet–Spinel Xenoliths from the Cenozoic Basalts of Mongolia. Isvestia AN SSSR, Ser. Geology, 5, pp. 36–58.

Kopylova, M.G., O'Reilly, S.Y., Genshaft, Yu.S., 1995. Thermal state of the lithosphere beneath Central Mongolia: evidence from deep-seated xenoliths from the Shavaryn–Saram volcanic centre in the Tariat depression, Hangai, Mongolia. Lithos 36, 243–255.

Kopylova, M.G., Nowell, G.M., Pearson, D.G., Markovic, G., 2009. Crystallization of megacrysts from protokimberlitic fluids: geochemical evidence from high-Cr megacrysts in the Jericho kimberlite. Lithos 112S, 284–295.

Kopylova, M.G., Beausoleil, Y., Goncharov, A., Burgess, J., Strand, P., 2016. Spatial distribution of eclogite in the slave cratonic mantle: the role of subduction. Tectonophysics 672–673, 87–103.

Krogh, E.J., 1988. The garnet–clinopyroxene Fe–Mg geothermometer - a reinterpretation of existing experimental data. Contributions to Mineralogy and Petrology 99, 44–48.

Kuligin, S.S., 1997. Complex of Pyroxenite Xenoliths in Kimberlites from Different Regions of Siberian Platform. PhD thesis. United Institute of Geology Geophysics and Mineralogy, Novosibirsk, 220 p.

Lavrent'ev, Yu G., Usova, L.V., Kuznetsova, A.I., Letov, S.V., 1987. X-ray spectral quantimetric microanalysis of the most important minerals of kimberlites. Russian Geology and Geophysics 48, 75–81.

Lazarov, M., Brey, G.P., Weyer, S., 2009. Time steps of depletion and enrichment in the Kaapvaal craton as recorded by subcalcic garnets from Finsch (SA). Earth and Planetary Science Letters 279, 1–10.

Logvinova, A.M., Taylor, L.A., Floss, C., Sobolev, N.V., 2005. Geochemistry of multiple diamond inclusions of harzburgitic garnets as examined in situ. International Geology Review 47, 1223–1233.

Malygina, E.V., 2000. Xenoliths of Granular Mantle Peridotites in Udachnaya Pipe. PhD thesis. United Institute of Geology Geophysics and Mineralogy, Novosibirsk, 220 p.

McGregor, I.D., 1974. The system $MgO–SiO_2–Al_2O_3$: solubility of Al_2O_3 in enstatite for spinel and garnet peridotite compositions. American Mineralogist 59, 110–119.

Metelkin, D.V., Kazansky, A.Yu., Bragina, V.Yu., Tsel'movich, V.A., Lavrenchuk, A.V., Kungurtseva, L.V., 2007. Paleomagnetism of the late Cretaceous intrusions from the Minusa trough (southern Siberia). Russian Geology and Geophysics 48, 185–198.

Mukhopadyay, B., 1991. Garnet–clinopyroxene geobarometry: the problems, a prospect, and an approximate solution with some applications. American Mineralogist 76, 512–529.

Nickel, K.G., 1989. Garnet–pyroxene equilibria in the system SMACCR (SiO_2–MgO–Al_2O_3–CaO–Cr_2O_3): the Cr-geobarometer. In: Ross, J. (Ed.), Kimberlites and Related Rocks, vol. 2, Their Mantle/crust Setting, Diamonds and Diamond Exploration. Proceedings of 4th International Kimberlite Conference. Geological Society of Australia Special Publication, 14, pp. 901–912.

Nickel, K.G., Green, D.H., 1985. Empirical geothermobarometry for garnet peridotites and implications for the nature of the lithosphere, kimberlites and diamonds. Earth and Planetary Science letters 73, 158–170.

Nimis, P., Taylor, W., 2000. Single clinopyroxene thermobarometry for garnet peridotites. Part I. Calibration and testing of a Cr-in-Cpx barometer and an enstatite-in-Cpx thermometer. Contributions to Mineralogy and Petrology 139, 541–554.

Nimis, P., Zanetti, A., Dencker, I., Sobolev, N.V., 2009. Major and trace element composition of chromian diopsides from the Zagadochnaya kimberlite (Yakutia, Russia): metasomatic processes, thermobarometry and diamond potential. Lithos 112, 397–412.

Nixon, P.H., Boyd, F.R., 1979. Garnet bearing lherzolites and discrete nodule suites from the Malaita alnoite, Solomon Islands, S.W. Pacific, and their bearing on oceanic mantle composition and geotherm. In: Boyd, F.R., Meyer, H.O.A. (Eds.), The Mantle Sample Inclusions in Kimberlite and other Volcanics. AGU, Wasington, pp. 400–423.

Ntaflos, T., Bjerg, E.A., Labudia, C.H., Kurat, G., 2007. Depleted lithosphere from the mantle wedge beneath Tres Lagos, southern Patagonia, Argentina. Lithos 94, 46–65.

O'Neill, H.St.C., Wall, V.J., 1987. The olivine orthopyroxene-spinel oxygen geobarometer, the nickel precipitation curve, and the oxygen fugacity of the Earth's upper mantle. Journal of Petrology 28, 1169–1191.

O'Neill, H.St.C., Wood, B.J., 1979. An experimental study of Fe-Mg- partitioning between garnet and olivine and its calibration as a geothermometer. Contributions to Mineralogy and Petrology 70, 59–70.

Ovchinnikov, Yu.I., 1990. Xenoliths from Obnazhennaya kimberlite pipe and alkali basalts from Minusa depression. Ph.D. dissertation Thesis. United Institute of Geology Geophysics, Mineralogy, Novosibirsk, 225 pp.

Pearson, D.G., Wittig, N., 2014. The Formation and Evolution of Cratonic Mantle Lithosphere – Evidence from Mantle Xenoliths In: Treatise on Geochemistry, second ed., vol. 3, pp. 255–292

Perkins, D., Newton, R.C., 1980. The compositions of coexisting pyroxenes and garnets in the system at $CaO–MgO–Al_2O_3–SiO_2$ at 900–1100 °C and high pressures. Contributions to Mineralogy and Petrology 75, 291–300.

Pokhilenko, L.N., 2006. Volatile Composition and Oxidation State of Mantle Xenoliths from Siberian kimberlites. PhD thesis. United Institute of Geology Geophysics and Mineralogy, Novosibirsk, 225 p.

Pokhilenko, N.P., Sobolev, N.V., Kuligin, S.S., Shimizu, N., 1999. Peculiarities of distribution of pyroxenite paragenesis garnets in Yakutian kimberlites and some aspects of the evolution of the Siberian craton lithospheric mantle. In: Proceedings of the VII International Kimberlite Conference. The P.H. Nixon Volume, pp. 690–707.

Pollack, H.N., Chapman, D.S., 1977. On the regional variations of heat flow, geotherms and lithospheric thickness. Tectonophysics 38, 279–296.

Reimers, L.F., 1994. Deep Seated Mineral Associations of the kimberlites Pipe Sytycanskaya (Materials of the Study of Mantle Rock and Crystalline Inclusions in Diamonds). Institute of Geology and Geophysics, Novosibirsk, 258 p.

Riches, A.J.V., Liua, Y., Day, J.M.D., Spetsius, Z.V., Taylor, L.A., 2010. Subducted oceanic crust as diamond hosts revealed by garnets of mantle xenoliths from Nyurbinskaya, Siberia. Lithos 120, 368–378.

Ryan, C.G., Griffin, W.L., 1996. Garnet geotherms: pressure–temperature data from Cr-pyrope garnet xenocrysts in volcanic rocks. Journal of Geophysical Research 101, 5611–5625.

Sen, G., 1988. Petrogenesis of spinel lherzolite and pyroxenite suite xenoliths from the Koolau shield, Oahu, Hawaii: implications for petrology of the post-eruptive lithosphere beneath Oahu. Contributions to Mineralogy and Petrology 100, 61–91.

Sen, G., Leeman, W.P., 1991. Iron-rich lherzolite xenoliths from Oahu: origin and implications for Hawaiian magma sources. Earth and Planetary Science Letters 102, 45–57.

Sharygin, I.S., Litasov, K.D., Shatskiy, A., Golovin, A.V., Ohtani, E., Pokhilenko, N.P., 2015. Melting phase relations of the Udachnaya-East Group-I kimberlite at 3.0–6.5 GPa: experimental evidence for alkali-carbonatite composition of primary kimberlite melts and implications for mantle plumes. Gondwana Research 28, 1391–1414.

Shatsky, V., Ragozin, A., Zedgenizov, D., Mityukhin, M., 2008. Evidence for multistage evolution in a xenolith of diamond-bearing eclogite from the Udachnaya kimberlite pipe. Lithos 105, 289–300.

Shatsky, V.S., Zedgenizov, D.A., Ragozin, A.L., Kalinina, V.V., 2015. Diamondiferous subcontinental lithospheric mantle of the northeastern Siberian Craton: evidence from mineral inclusions in alluvial diamonds. Gondwana Research 28, 106–120.

Shirey, S.B., Carlson, R.W., Richardson, S.H., Menzies, A., Gurney, J.J., Pearson, D.G., Harris, J.W., Wiechert, U., 2001. Archean emplacement of eclogitic components into the lithospheric mantle during formation of the Kaapvaal Craton. Geophysical Research Letters 28, 2509–2512.

Simakov, S.K., 2008. Garnet–clinopyroxene and clinopyroxene geothermobarometry of deep mantle and crust eclogites and peridotite. Lithos 106, 125–136.

Skewes, M.A., Stern, C.R., 1979. Petrology and geochemistry of alkali basalts and ultramafic inclusions from the Pali–Aike volcanic field in southern Chile and the origin of the Patagonian plateau lavas. Journal of Volcanology and Geothermal Research 1–2, 3–25.

Sobolev, N.V., Lavrent'ev, Yu.G., 1971. Isomorphic sodium admixture in garnets formed at high pressures. Contributions to Mineralogy and Petrology 31, 1–12.

Sobolev, N.V., Pustyntsev, V.I., Kuznetsova, I.K., Khar'kiv, A.D., 1970. New data on the mineralogy of the diamond-bearing eclogites from the "Mir" pipe (Yakutia). International Geology Review 12, 657–659.

Sobolev, N.V., Lavrentev, Y.G., Pokhilenko, N.P., Usova, L.V., 1973. Chrome-rich garnets from the kimberlites of Yakutia and their parageneses. Contributions to Mineralogy and Petrology 40, 39–52.

Sokol, A.G., Kruk, A.N., Chebotarev, D.A., Palyanov, Y.N., 2016. Carbonatite melt–peridotite interaction at 5.5–7.0 GPa: implications for metasomatism in lithospheric mantle. Lithos 248–251, 66–79.

Sobolev, V.N., Taylor, L.A., Snyder, G.A., Sobolev, N.V., 1994. Diamondiferous eclogites from the Udachnaya pipe, Yakutia. International Geology Review 36, 42–64.

Spetsius, Z.V., 2004. Petrology of highly aluminous xenoliths from kimberlites of Yakutia. Lithos 77, 525–538.

Spetsius, Z.V., Taylor, L.A., Valley, J.W., Ivanov, A.S., Banzeruk, V.I., 2008. Diamondiferous xenoliths from crustal subduction: garnet oxygen isotopes from the Nyurbinskaya pipe, Yakutia. European Journal of Mineralogy 20, 375–385.

Stern, C.R., 1991. Mantle Xenoliths from the Quaternary Pali–Aike Volcanic Field of Southernmost South America: Implications for the Accretion of Phanerozoic Continental Lithosphere. Extended Abst. 5th IKC, p. 395.

Please cite this article in press as: Ashchepkov, I.V., et al., Monomineral universal clinopyroxene and garnet barometers for peridotitic, eclogitic and basaltic systems, Geoscience Frontiers (2016), http://dx.doi.org/10.1016/j.gsf.2016.06.012

Stern, C.R., Kilian, R., Olker, B., Hauri, E.H., Kyser, T.K., 1999. Evidence from mantle xenoliths for relatively thin 100 km continental lithosphere below the Phanerozoic crust of southernmost South America. Lithos 48, 217–235.

Taylor, W.R., 1998. An experimental test of some geothermometer and geobarometer formulations for upper mantle peridotites with application to the thermobarometry of fertile lherzolites and garnet websterite. Neues Jahrbuch für Mineralogie Abhandlungen 172, 381–408.

Tsai, H.M., Meyer, H.O.A., Moreau, J., Milledge, J., 1979. Mineral inclusions in diamond: Premier, Jagerfontein and Finsch kimberlites, South Africa, and Williams mine, Tanzania. Proceedings of the 2nd International Kimberlite Conference. American Geophysical Union 2, 16–26.

Turkin, A.I., Sobolev, N.V., 2009. Pyrope–knorringite garnets: overview of experimental data and natural parageneses. Russian Geology and Geophysics 50, 1169–1182.

Viljoen, F., Dobbe, R., Harris, J., Smit, B., 2010. Trace element chemistry of mineral inclusions in eclogitic diamonds from the premier (Cullinan) and Finsch kimberlites, South Africa: implications for the evolution of their mantle source. Lithos 118, 156–168.

Wang, J., Hattori, K.H., Li, J., Stern, C.R., 2008. Oxidation state of Paleozoic subcontinental lithospheric mantle below the Pali Aike volcanic field in southernmost Patagonia. Lithos 105, 98–110.

Wang, C., Jin, Z.-M., Gao, S., Zhang, J.-F., Zheng, S., 2010. Eclogite-melt/peridotite reaction: experimental constrains on the destruction mechanism of the North China Craton. Science China Earth Sciences 53, 797–809.

Wells, P.R., 1977. Pyroxene thermometry in simple and complex systems. Contributions to Mineralogy and Petrology 62, 129–139.

Wu, C.M., Zhao, G., 2011. The applicability of garnet–orthopyroxene geobarometry in mantle xenoliths. Lithos 125, 1–9.

Xu, X., O'Reilly, S.Y., Zhou, X., Griffin, W.L., 1996. A xenolith-derived geotherm and the crust–mantle boundary at Qilin, southeastern China. Lithos 38, 41–62.

Xu, X., O'Reilly, S.Y., Griffin, W.L., Zhou, X., 2003. Enrichment of upper mantle peridotite: petrological, trace element and isotopic evidence in xenoliths from SE China. Chemical Geology 198, 163–188.

Yaxley, G.M., Berry, A.J., Kamenetsky, V.S., Woodland, A.B., Golovin, A.V., 2012. An oxygen fugacity profile through the Siberian Craton — Fe K-edge XANES determinations of $Fe^{3+}/\sum Fe$ in garnets in peridotite xenoliths from the Udachnaya East kimberlite. Lithos 140–141, 142–151.

Zheng, J., Griffin, W.L., O'Reilly, S.Y., Liou, J.G., Zhang, R.Y., Lu, F., 2010. Late mesozoic–eocene mantle replacement beneath the eastern North China craton: evidence from the Paleozoic and Cenozoic peridotite xenoliths. International Geology Review 47, 457–472.

Ziberna, L., Nimis, P., Zanetti, A., Sobolev, N.V., 2013. Metasomatic processes in the Central Siberian cratonic mantle: evidence from garnet-xenocrysts from the Zagadochnaya kimberlite. Journal of Petrology 54, 2379–2409.

Please cite this article in press as: Ashchepkov, I.V., et al., Monomineral universal clinopyroxene and garnet barometers for peridotitic, eclogitic and basaltic systems, Geoscience Frontiers (2016), http://dx.doi.org/10.1016/j.gsf.2016.06.012